Appendix E

Stream Inspection Documents

Stream Inspection Proforma Summary

Station	1	2	3	4	5	6	7	12	14	19	21	25	30	Macquarie River
Station Description	Summer Hill Creek	NB	Summer Hill Trib	NB	Summer Hill Creek	NB	Drainage Depression	Oky Creek	Oky Creek Trib	NB	Trib Summer Hill	Oky Creek RHS	Drainage Depression	Macquarie River
Way Points	1 - right bank; 2 BR LHS; 3 BR RHS	4 - BR RHS; 5 - BR LHS	16- Culv LHS Top; 17 - Culv RHS Top; 18 - WL	7 - BR LHS; 8-BR RHS;11 - RT Bank;12 - LF Bank;13- LHS d/s BR;14- RHS d/s BR; 15 - TOC	27- RHS Culv; 28 - LHS Culv; 29 - WL D/B LHS; 30 WL u/s RHS; 31 to 36 - Spring CL	37 - HC; 38 - 1L Culv; 39 - LHS u/s; 40 RHS u/s; 41 d/s of bank erosion LHS;	Photo	NB	75 - RHS d/s; 76 LHS d/s	19 - Top d/s; 20 - Inv u/s;21 - Top u/s;22- Top Head cut;23- top	24 - RHS Inv d/s; 25 LHS Inv d/s; 26 - Top Culv		72 - Culv RHS;73-Culv LHS;74 - Invert	Photos - Ecology Camera
Pattern	Straight	Straight	Meandering	Meandering	Meandering	Meandering	Meandering	Meandering	Straight	NB		Meandering	Meandering	Meandering
Primary Bed Material	Slit Clay	Slit Clay	Slit Clay	Slit Clay	Gravel;Slit Clay	Cobble;Gravel;Silt Clay	Slit Clay	Bedrock;Gravel;Silt clay	Boulder/Cobble;Silt Cla	Bedrock;Gravel	Bedrock;Boulder/Cobble;Silt Cla	Boulder/Cobble;Silt Clay	Boulder/Cobble;Silt Clay	Bedrock
Bed/bank Protection	No	No	No	No	Yes	NB	No	No	No	2 Banks	Yes	No	Yes - Downstream; No - U	Yes
Degree of Incision	11-25%	11-25%	26-50%	0-10%	0-10%	NB	26-50%	0-10%	26-50%	0-10%	11-25%	0-10%	51-75%	0-10%
Degree of Constriction	NB	0-10%	11-25%	26-50%	26-50%	NB	0-10%	0-10%	0-10%	0-10%	0-10%	0-10%	0-10%	76-100%
Streambank Erosion														
Left	fluvial	fluvial	fluvial	fluvial	None	fluvial	fluvial	fluvial	fluvial	fluvial	None	fluvial	fluvial	None
Right	None	fluvial	fluvial	fluvial	None	fluvial	fluvial	mass wasting	fluvial	fluvial	None	fluvial	fluvial	None
Streambank Instability														
Left	11-25%	0-10%	11-25%	0-10%	0-10%	26-50%	11-25%	11-25%	51-75%	0-10%	0-10%	0-10%	0-10%	0-10%
Right	11-25%	0-10%	26-50%	0-10%	0-10%	26-50%	11-25%	51-75%	51-75%	0-10%	0-10%	0-10%	0-10%	0-10%
Established ripirian woody vegetative cover														
Left	0-10%	11-25%	0-10%	0-10%	51-75%	0-10%	0-10%	26-50%	11-25%	26-50%	11-25%	26-50%	0-10%	26-50%
Right	0-10%	0-10%	0-10%	0-10%	51-75%	0-10%	0-10%	51-75%	11-25%	26-50%	11-25%	0-10%	0-10%	26-50%
Occurrence of Bank accretion														
Left	11-25%	11-25%	NB	26-50%	51-75%	0-10%	0-10%	11-25%	0-10%	11-25%	0-10%	26-50%	11-25%	26-50%
Right	11-25%	11-25%	NB	26-50%	51-75%	0-10%	0-10%	11-25%	0-10%	11-25%	0-10%	0-10%	11-25%	26-50%
Composition of adjacent side slope														
Left	Fines	Fines	Gravel SP ; Fines	Gravel SP	Bedrock;Boulders;Gravel SP	Gravel SP ; Fines	Gravel SP ; Fines	Gravel SP	Fines	Bedrock;Gravel SP	Boulders;Gravel SP	Gravel SP	Boulders;Gravel SP	Bedrock;Fines
Right	Fines	Fines	Gravel SP ; Fines	Bedrock;Boulders;Gravel SP	Bedrock;Boulders;Gravel SP	Gravel SP ; Fines	Gravel SP ; Fines	Bedrock;Gravel SP	Fines	Bedrock;Gravel SP	Boulders;Gravel SP	Bedrock;Fines	Boulders;Gravel SP	Bedrock;Fines
Severity of side-slope erosion														
Left	Low	Low	High	None	None	Moderate	Low	Low	NB	None	None	Low	None	Low
Right	Low	Low	High	None	None	Moderate	Low	High	NB	None	None	Low	None	None
Baseflows	10.20 L/s	20L/s Turbid, confined	5 L/s	50-100 L/s	50-100 L/s	5 L/s	none	5 L/s	None	None (Trickle)	5 L/s	10 L/s	none	100ML/day
Weeds	Prickly pear;Willows;Blackberry;kikuyu	Prickly pear;Willows;Blackberry;kikuyu	Prickly pear;Willows;Blackberry;kikuyu;Carex	Willows;Carex;White bulb on weed; Purple Thistle	Thorns	Blackberry;Kikuyu;Carex;Thorns	Kikuyu;Carex	Blackberry; Thorns	No Weeds	Blackberry;Kikuyu	Blackberry;Native Grasses;Wattle;Lomandra	Blackberry; Thorns	Willows; Typha	Prickly Pear;Willows;Blackberry;Kikuyu;Tiger pear
NOTES/COMMENTS														

Stream Crossing Photos

Stream Crossing 1: Ophir Road crossing Summer Hill Creek

Figure 1: Looking downstream from Ophir Road bridge. Note the highly turbid flow near the left bank at the confluence with Blackmans Swamp Creek. There is substantial in-stream vegetation, with silt & clay bed material. Tree stumps are remnants of previously removed willow trees.

Figure 2: Looking upstream from Ophir Road bridge, similar in-stream vegetation, though note the left bank (in a downstream direction) is devoid of trees/deep rooted vegetation.

Stream Crossing 2: Ophir Road crossing Summer Hill Creek

Figure 3: Looking downstream at Crossing 2. The banks are well vegetated, though the channel width is a lot smaller than for Crossing 1, resulting in higher velocity flow. Sit and Clay bed material with little deep rooted vegetation/trees.

Stream Crossing 3: Ophir Creek crossing Unnamed Creek

Figure 4: Downstream side of existing Ophir Road culvert. Small unnamed creek with a wide flowpath results in shallow flow depth. Well vegetated in-stream with grasses with silt and clay bed/bank material, no deep rooted vegetation or trees on banks.

Stream Crossing 4: Ophir Road crossing Summer Hill Creek

Figure 5: Looking upstream from Ophir Road bridge, wide flowpath results in low velocity flow. Right bank well vegetated with shrubs and trees, sparse vegetation on left bank with some areas of exposed silt and clay.

Figure 6: Looking downstream from Ophir Road bridge. Narrowing channel results in high velocity flow. Left bank poorly vegetated and right bank abuts a valley wall with exposed bedrock.

Stream Crossing 19: Ophir Road crossing Unnamed Creek

Figure 7: Looking downstream from Ophir Road. Creek bed composed of exposed bedrock interspersed with exposed silt and clay, and grassed sections, leaving it erodible if disturbed.

Stream Crossing 21: Ophir Road crossing Cow Creek

Figure 8: Looking upstream of Ophir Road. Well vegetated with grasses and shrubs on upper banks upstream and downstream of Ophir Road with narrow well defined channel with steep but vegetated bank faces.

Figure 9: Looking at right bank on downstream side of Ophir Road. Note the bed material of Cow Creek grading from cobblestones, gravel, silt, and clay.

Stream Crossing 5: Ophir Road crossing Summer Hill Creek

Figure 10: Looking downstream from Ophir Road. Creek channel controlled by bedrock with pockets of deposited gravel, silt and clay.

Figure 11: Upstream side of Ophir Road, wider channel than downstream with well vegetated left bank and gravel deposits on right bank.

Stream Crossing 6: Ophir Road crossing Kitty's Creek

Figure 12: Looking downtream from Ophir Road stream channel controlled by bedrock with gravel deposits in-stream.

Figure 13: Looking upstream from Ophir Road at head-cut and plunge pool, most likely a result of the road corssing construction changing the bed level and hydrology of the creek.

Stream Crossing 7: Lookout Road crossing Unnamed Creek

Figure 14: Looking downstream from Lookout Road. Well grassed shallow channel with a silt and clay bed material.

Figure 15: Looking upstream from Lookout Road. Gully formations at least 100m upstream of the road culverts obvious sign of previous bank erosion. The creek channel appears to have restabilised.

Stream Crossing 12: Lookout Road crossing Oaky Creek

Figure 16: Looking downstream, from a pool at the causeway crossing, note the small riffle dowsntream. Steep upper bank slopes were observed in the back ground indicating bank erosion at high stage.

Figure 17 Right bank face. Exposed bank with active signs of erosion most likely a result of stock access to creek.

Stream Crossing 25: Lookout Road crossing Oaky Creek

Figure 18 View from the left top of bank. Note the creek bed mainly composed of cobblestones with gentle bank faces lined with large casuarina trees.

Stream Crossing 14: Lookout Road crossing Unnamed Creek

Figure 19 Looking downstream from Lookout Road, note the bed composition of cobblestones, pebbles, and silt. Upper banks comprise of silt/clay soil and grasses.

Figure 20 Looking to the right bank from the left. Note the road surface is integrated into the creek bed. Note the slight grading up to top of banks and exposed soil on upper bank.

Stream Crossing 30: Long Point Road crossing Unnamed Creek

Figure 21 Downstream side of Long Point Road looking from left bank to right. Note the channel material of bedrock, boulders, silt & clay with in-stream vegetation and grasses/shrubs on the banks.

Figure 22 Upstream of Long Point Road looking from left bank. Channel controlled by bedrock with silt/clay overburden. Exotic vegetation present in the channel.

Appendix F

3D Reservoir Modelling Report

Cardno (NSW/ACT) Pty Ltd
ABN 95 001 145 035

Level 9 The Forum
203 Pacific Highway
St Leonards NSW 2065
Australia

Telephone: 02 9496 7700
Facsimile: 02 9439 5170
International: +61 2 9496 7700

sydney@cardno.com.au
www.cardno.com.au

Document Control:

Version	Status	Date	Author		Reviewer	
			Name	Initials	Name	Initials
1	FINAL	23 May 2012	Doug Treloar	PDT	Cedric Phocas	CP

TABLE OF CONTENTS

TABLES

FIGURES

1 INTRODUCTION

1.1 Model System Requirements

Numerical modelling of the existing and future thermo-hydrodynamic processes in the reservoir required the application of a numerical model with the capability to describe 3D current and density structures and to appropriately handle the heat processes (solar radiation and water column penetration of heat), vertical mixing, meteorological variations, net evaporation/rainfall/seepage flows, wind forcing and influx/efflux caused currents.

In this case it was decided that the Delft3D model should be used. A succinct description follows.

2 MODEL SYSTEM

For the purposes of this study it was decided to use the Delft3D modelling system so that 3D spatial current speeds and temperature variation could be described. This is important because, apart from the immediate momentum of the catchment inflows to the reservoir, and the overall circulation structure developed between the inflows and off-take flow, the principal current forcing mechanism (and cooling mechanism) is wind.

Wind driven currents are caused by inter-facial shear between the wind and lake surface. An appropriate wind friction factor, varying with wind speed, relates wind speed to shear stress, and then to the transfer of vorticity to the water column. This vorticity disperses down through the water column, gradually accelerating the whole flow. However, the maximum wind-caused current will normally be at the surface, with zero current near the lake bed, because of bed friction. In enclosed lakes, such as the Suma Park reservoir system, upper water column currents are normally in the direction of the wind, with more complex return flows at depth. However, wind driven currents at the bed may also be in the direction of the wind in shallower, nearshore areas because the wind shear force per unit volume of water is greater there, and in the direction opposite to the wind at the surface in deeper water. Hence a much more physically realistic current field can be modelled with a 3D model system such as Delft3D.

Additionally, inflow water may be more or less buoyant than ambient lake water and will tend to form a sinking or surface plume. This will also be dependent on wind conditions, which, when sufficiently strong, cause significant mixing throughout the water column. When wind speed abates the stratification can reform. Generally, the shallow water of shoreline areas and the higher effective bed friction of those areas lead to well mixed, nearly constant temperatures throughout the water column; whereas deeper areas will show more seasonal stratification.

Delft3D also includes a heat flux model with cooling caused by wind speed, surface area and relative water to air temperature difference. Moreover, solar radiation is included, with the heat/depth penetration algorithm being affected by light penetration described by a model Secchi depth parameter (constant throughout the model domain). Cloud cover (estimated) and relative humidity are also required input parameters.

A model of the reservoir was set up using the bathymetric data available from Orange City Council and supplied on 15 February 2012. **Figure 2.1 and 2.2** show a general view of the model grid and bathymetry developed for this study, as well as the locations of the inflows and outflows.

In order to resolve the vertical current, temperature and density structure, ten vertical water column layers were modelled. Delft3D uses a sigma coordinate system, which means that in this case depth is divided into ten layers. Layer thicknesses were equally spread and set to be 10% of the depth. This vertical structure allows the realistic description of the vertical variation of horizontal currents and temperature/density.

Density differences are included in the model so that the warmer/cooler inflows may form surface or sinking plumes until they are mixed through the water column. Horizontal density gradients also affect the flow structure.

Horizontal solution is undertaken using the Alternating Direction Implicit (ADI) method of Leendertse for shallow water equations. In the vertical direction (in 3D mode) a fully implicit time integration method is applied.

Vertical turbulence closure in Delft3D is based on the eddy viscosity concept. A k-ε vertical turbulence model was adopted in the 3D simulations undertaken for this study.

Near shore areas have moving water lines as the lake fills and empties; consequently Delft3D includes a robust and efficient wetting and drying algorithm to handle this process. Generally wetting and drying were not important to this study, but near shore water depths were affected significantly by changing water levels (up to 12m water level variation from wet to dry periods).

Delft3D provides the facility to adopt a modelling approach known as domain decomposition – known also as parallel processing. Domain decomposition is a technique in which a model is divided into several smaller model domains with finer grids. The subdivision is based on the horizontal and vertical model resolution required for adequately describing physical processes in some areas; whereas other areas where the depths and processes have less spatial variation require less resolution. Then, the computations can be carried out dynamically on these domains. The communication between the domains takes place along internal boundaries, or so-called DD-boundaries. Computations are carried out concurrently, that is via parallel computing, thus reducing the turnaround time of multiple domain simulations. Domain decomposition allows for local grid refinement, both in the horizontal direction and in the vertical direction. Grid refinement in the horizontal direction means that in one domain smaller mesh sizes are used than in other domains. In the case of vertical grid refinement, one domain, for example, may use ten vertical layers whilst another domain may use five layers, or a single layer (depth-averaged).

Domain decomposition is widely recognised as an efficient and flexible tool for the simulation of complex physical processes in spatially variable bathymetric conditions.

The model grid system was prepared with the main objective of having high resolution near the off-take, but it also needed to describe a large area in order to accurately represent the flow structure variations and heat storage and flux.

A coarse grid with a grid size of 90m is linked to a finer grid with a 1 to 3 ratio. Hence, the grid size of the refined grid is 30m. The grids are linked dynamically in the model. This model system allowed a significant reduction of the duration of the simulations without reducing the resolution of the results and processes in the area of interest; that is, the dam off- take and the inflow from the pipeline.

3 DATA

A range of data items were required to set up and verify the model, and then undertake a set of scenario simulations. Data from the Orange airport on-site weather station were provided for both the verification and scenario simulation periods by the Bureau of Meteorology. The available recorded solar radiation data came from Wagga Wagga airport, which was the closest available data to the site.

3.1 Lake Depth Data

This information is required to numerically describe the plan outline of the lakes edges and the variation of depth throughout the lake. It was developed using the bathymetry information provided by Orange City Council on 15 February 2012. The Delft3D model was set up with all depths relative to the spillway crest level (FSL).

3.2 Wind Data

A realistic description of the seasonal time varying wind field is needed by the model to ensure realistic lake currents and cooling – calibration and design simulation cases. This data was provided by the Bureau of Meteorology for Orange airport. About 16 years of data were available. It was applied as a uniform wind field to the model. **Figure 3.1** provides a wind rose that describes the annual wind speed and direction joint occurrence.

3.3 Reservoir in-Flow Data

This data was taken from reservoir water balance modelling undertaken by Geolyse, and referred to in Section 3 of the main report.

3.4 Water Quality Data

Water quality data has been provided by GHD at different stations within the region around Suma Park Reservoir. Data from station 421051was used to estimate the water temperature of the Suma Park catchment and the stormwater harvest flows. Station 421025 data was used for the Macquarie River flow.

The flow and temperature data is described in **Figure 3.2**.

3.5 Meteorological Data

The heat flux module of Delft3D requires spatially uniform time-series information describing solar radiation in Watts/m^2 and relative humidity, as well as air temperature data. This information was provided by a site at Wagga Wagga in MJ/m^2.

This solar radiation data was available at hourly intervals and provided a reliable description of diurnal variation as shown in **Figure 3.3a**. Due to gaps in the data, the solar radiation has been averaged as monthly data. It means, for example, that each day of January will have a similar diurnal cycle as described by **Figure 3.3b**, and that the data is a general year rather than a specific year.

Time series of air humidity and temperature were available but were too irregular with many data gaps to be used. Hence, monthly data from the BOM at Orange airport were used. Averaged maximum and minimum air temperature data are available for each month based on data from 1996 to 2012 (see **Figure 3.4)**. Averaged relative humidity at 9AM and 3PM are available for each month based on data from 1996 to 2012 as shown on **Figure 3.4**.

These data were used to recreate the diurnal cycle. As previously stated, each day of January will have the same diurnal cycle with an hour time step. The variations were specified to have the lowest daily temperature at 5am and the highest daily temperature at 2pm.

3.6 Reservoir Temperatures

Temperature profiles near the off-take (about 17m deep) were provided by GHD. They were taken at irregular intervals throughout the year over the period from 2004 to 2011. This data was analysed to provide a generalised annual description of monthly near surface and near lake bed temperatures, see **Figure 3.5**. The records were too irregular and sparse to be applied to any specific year. The results show a distinct seasonal character, with stratification being evident in the summer months and being practically absent during winter.

It is noted that diurnal variations in surface temperature could not be described by this data.

4 MODEL CALIBRATION

Confidence in the outcomes of model simulations is increased when the system is verified and model parameters calibrated against recorded on-site data. After a number of trials, verification was undertaken by simulating a general period of one year. Specific year case data was not available because of the sparse records and different years of records.

Scaling of wind speed was required to achieve good performance from the model – noting that the terrain at the reservoir is different from that at Orange Airport. This task involved a number of simulations in which initial lake temperature was varied, and/or variations in wind friction factor and adjustment of the horizontal eddy diffusivity were made.

All of these variations were made keeping the parameters within physically realistic ranges, some of which are described below:

- 'Initial' lake temperature distribution throughout the lake is not known for the start of each simulation. This condition was therefore tested so that at the end of one year of simulation the top and bottom water temperatures were similar to those observed in the field and to the start temperatures.
- Wind friction factor was found to not have a major influence on currents and temperatures.
- Although recorded solar radiation is likely to be relatively realistic, the model 'sees' the radiation as a net heat input that typically requires some adjustment. Furthermore, the only available data was measured as net solar radiation, which differs from the measure that the Delft3D model requires. The Secchi depth parameter was set to 1m to assist with stratification verification.
- Vertical eddy viscosity was set using the k–ε turbulence model physically most realistic. Horizontal eddy viscosity was set at 0.15m^2/s. This is very small, but it was found to also affect vertical mixing and horizontal currents in the reservoir are generally very low. Hence this was a verification outcome.
- Air temperature from Orange airport were increased by 2°C to match the water surface temperature in the reservoir.

It is important to note that many of these parameter changes have non-linear consequences. Hence, about twenty verification runs were required to achieve acceptable agreement between the modelled and recorded data – typically a variation of ≤ 1.0^oC was sought, in line with what is considered to be the model accuracy.

Figure 4.1 plots the model time-series at the off-take field-measurement location for both the surface and near bed layers, and makes comparisons with the generalized field measurements recorded over a period of several years. This comparison shows that the shape of the modelled annual lake temperatures is realistic and that the summer-winter difference in stratification is described well. Surface temperatures show more variation in the period from August to March than April to June.

5 RESULTS

The calibrated model was used to investigate the potential influence of contaminants in the Macquarie River on water quality at the off-take. In these analyses three conservative marker contaminants were set at 100 in each of the three inflows – Stormwater Harvest, Suma Park catchment and the Macquarie River. This approach allowed the separate identification of contaminants originating from each source to be tracked – as may be required. A period of two years from July 1996 to July 1998 was selected for analysis. During this period Macquarie River flows were relatively high with respect to the Suma Park catchment flows. A simple box model approach was used with the available flow data (average annual flows), to estimate realistic initial concentrations for each of the three marker contaminants. That analysis also showed that a significant change in inflows requires about 1.5 years to affect the whole reservoir.

Figure 5.1 illustrates the outcome of this analysis and shows that the concentrations of Suma Park and Stormwater Harvest contaminants are reduced by introducing the Macquarie River flows. These results have been combined with contaminant data from each source to describe the change in four selected contaminants that would be caused by this extra inflow for the selected analysis period.

Figure 5.2 shows the effect of the Macquarie River inflows in terms of the depth-averaged 95th percentile high concentration of marker contaminant entering from that river. There is no identifiable effect at the Reservoir off-take. **Figure 5.3** shows that this also the case in terms of all of the ten layers applied in this numerical modelling work.

A simplified pollutant mass balance was undertaken based on the concentrations of each of the three input locations to the reservoir. This analysis is simplified in that there is no decay or water quality processes incorporated. For example, there is no die-off of E-coli modelled in this process. Instead, the average concentrations for each water quality parameter are applied to the conservative tracers (or representative concentration from each inflow point) to determine an overall concentration at various points within the reservoir.

The results of this tracer analysis have been applied to four key water quality parameters of interest:

- Bromide – due to the importance of this parameter in terms of the treatment process.
- Total Nitrogen & Total Phosporous – to determine the potential for algal blooms to form at certain areas in the reservoir
- E.Coli – based on likely human health impacts, both within the reservoir and the treatment process.

Table 5-1 shows the average concentration of the four parameters in the inflows used in the tracer analysis. It should be noted that the inflow water quality data was too sparse and irregular to use a time series of inflow concentrations. This data was then combined with the 95th percentile tracer percentage at the locations shown in **Figure 5.4.** The individual contributions from each source were combined using a weight based on the proportion of marker contaminant contributed to the total 95th percentile tracer percentage.

Table 5-1 Average of Concentration of Main Pollutants at Inflows

	Suma Park Catchment	Macquarie River Drought Relief	Stormwater Harvest
Bromide (mg/L)	0.07	0.09	0.02
Total Nitrogen (mg/L)	0.60	0.74	0.94
Total Phosphorus (mg/L)	0.05	0.04	0.05
E.Coli (CFU/L)	3000	650	120

Table 5.2 presents the 95th percentile concentration at the locations in **Figure 5.4** for each of the four parameters. The results generally compare well with that of the preliminary mass balance, indicating no major increases in concentration with Macquarie River pumping. The spatial variation in the 95th percentile concentration is also not significant across all parameters, except near the discharge location (see **Table 5.2** and **Figure 5.4).** Parameter concentrations near the discharge location tend to increase more than other locations in the reservoir (as would be expected).

Bromide is unlikely to impact on the environmental health of the reservoir, with the primary impact potentially on the treatment plant. Only a small increase is observed at the Reservoir Off-take and the treatment plant should be capable of withstanding these small increases in Bromide.

There are only small increases in concentrations in nutrients throughout the reservoir. However, as noted, there are complex processes of algal growth that affect nutrient concentrations that are not incorporated in this analysis. However, the analysis indicates that the nutrient concentrations would not be significantly different to the existing scenario, and therefore the risk of algal blooms is unlikely to be significantly higher.

The exception to this is near the discharge point from the pipeline. In the immediate vicinity of the discharge point, there is the potential for a localised increase in nutrient concentrations, particularly total nitrogen. This may result in a higher localised risk to algal blooms in this particular area.

The expected increases in e-coli concentrations are relatively minor, and therefore are not expected to represent a significant increase in risk to the reservoir. As noted above, it is expected that these concentrations are conservative as the exposure to UV light and other processes will result in lower concentrations of e-coli.

Table 5-2a 95% ile Results at various locations in the reservoir – Bromide (mg/L)

	Model without Macquarie River Inflow	Model with Macquarie River Inflow
Suma Park Catchment Inflow	0.07	0.08
Stormwater Harvest	0.07	0.08
Discharge	0.06	0.13
Reservoir	0.07	0.08
Reservoir Offtake	0.06	0.08

Table 5-2b 95% ile Results at various locations in the reservoir – Total Nitrogen (mg/L)

	Model without Macquarie River Inflow	Model with Macquarie River Inflow
Suma Park Catchment Inflow	0.65	0.70
Stormwater Harvest	1.06	0.98
Discharge	0.64	1.15
Reservoir	0.66	0.76
Reservoir Offtake	0.66	0.77

Table 5-2c 95% ile Results at various locations in the reservoir – Total Phosphorus (mg/L)

	Model without Macquarie River Inflow	Model with Macquarie River Inflow
Suma Park Catchment Inflow	0.05	0.06
Stormwater Harvest	0.07	0.07
Discharge	0.05	0.08
Reservoir	0.05	0.06
Reservoir Offtake	0.05	0.06

Table 5-2d 95% ile Results at various locations in the reservoir – E.Coli (CFU/L)

	Model without Macquarie River Inflow	Model with Macquarie River Inflow
Suma Park Catchment Inflow	3010	3050
Stormwater Harvest	2740	2770
Discharge	2690	3120
Reservoir	2700	2790
Reservoir Offtake	2690	2790

Figures

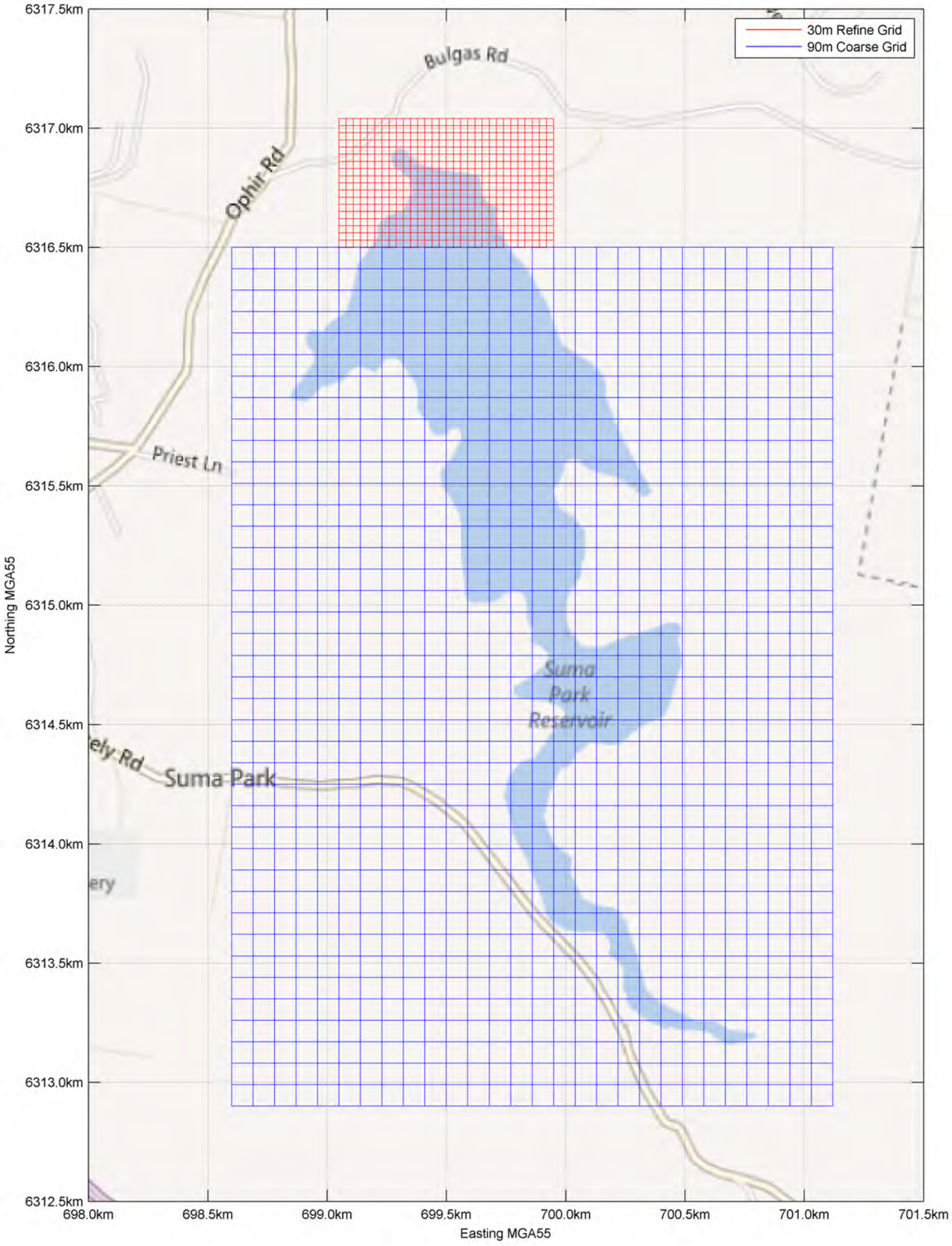

Suma Park Reservoir Numerical Modelling of the Hydro−Thermal Processes and Additional Influx

Cardno

Grid Setup
Coarse and Refined Grids
Figure 2.1

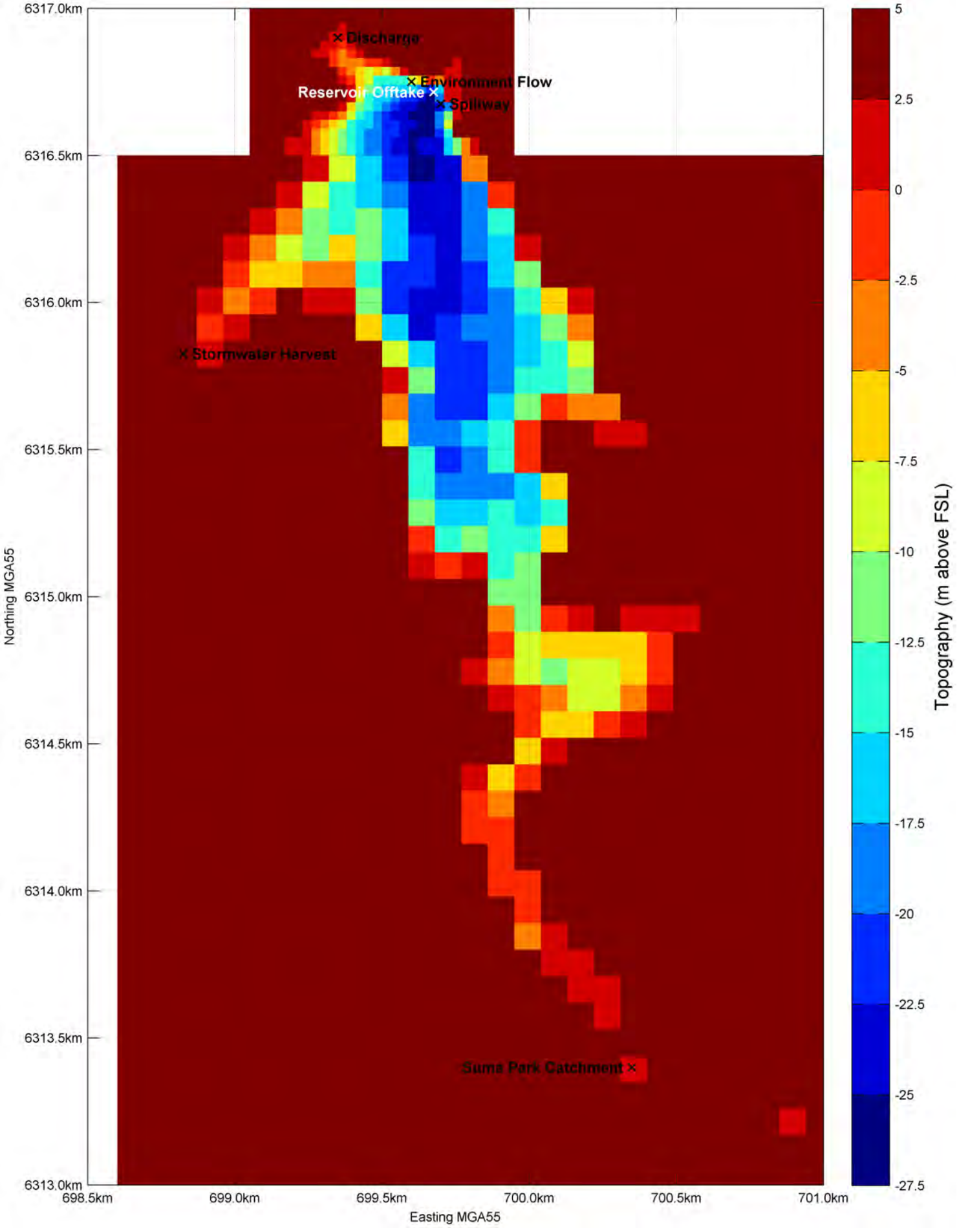

Suma Park Reservoir Numerical Modelling of the Hydro−Thermal Processes and Additional Influx

Cardno

Model Bathymetry
Inflow and Outflow Locations
Figure 2.2

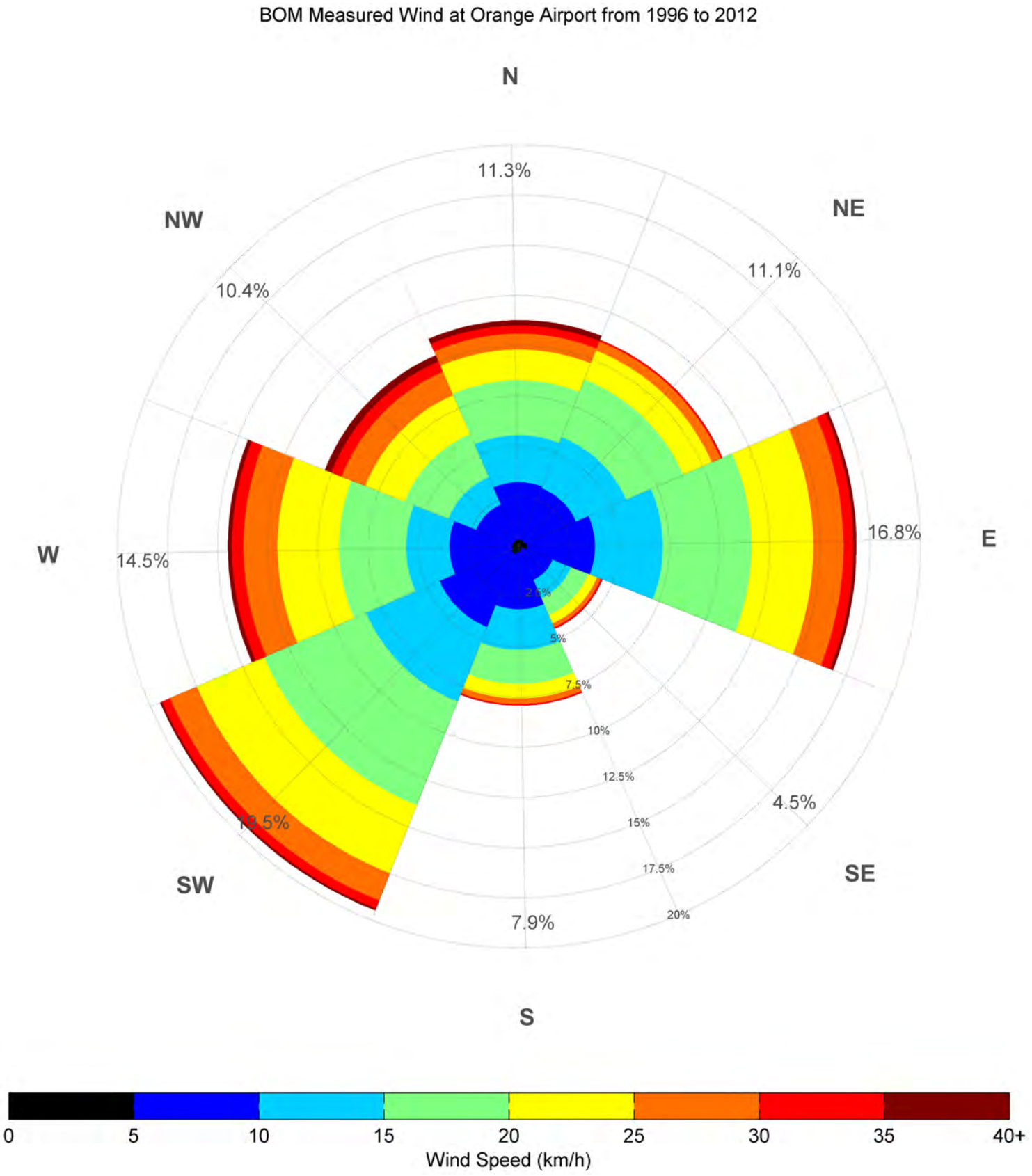
BOM Measured Wind at Orange Airport from 1996 to 2012
N
NE
E
SE
S
SW
W
NW
11.3%
11.1%
16.8%
4.5%
7.9%
19.5%
14.5%
10.4%
2.5%
5%
7.5%
10%
12.5%
15%
17.5%
20%
0
5
10
15
20
25
30
35
40+
Wind Speed (km/h)

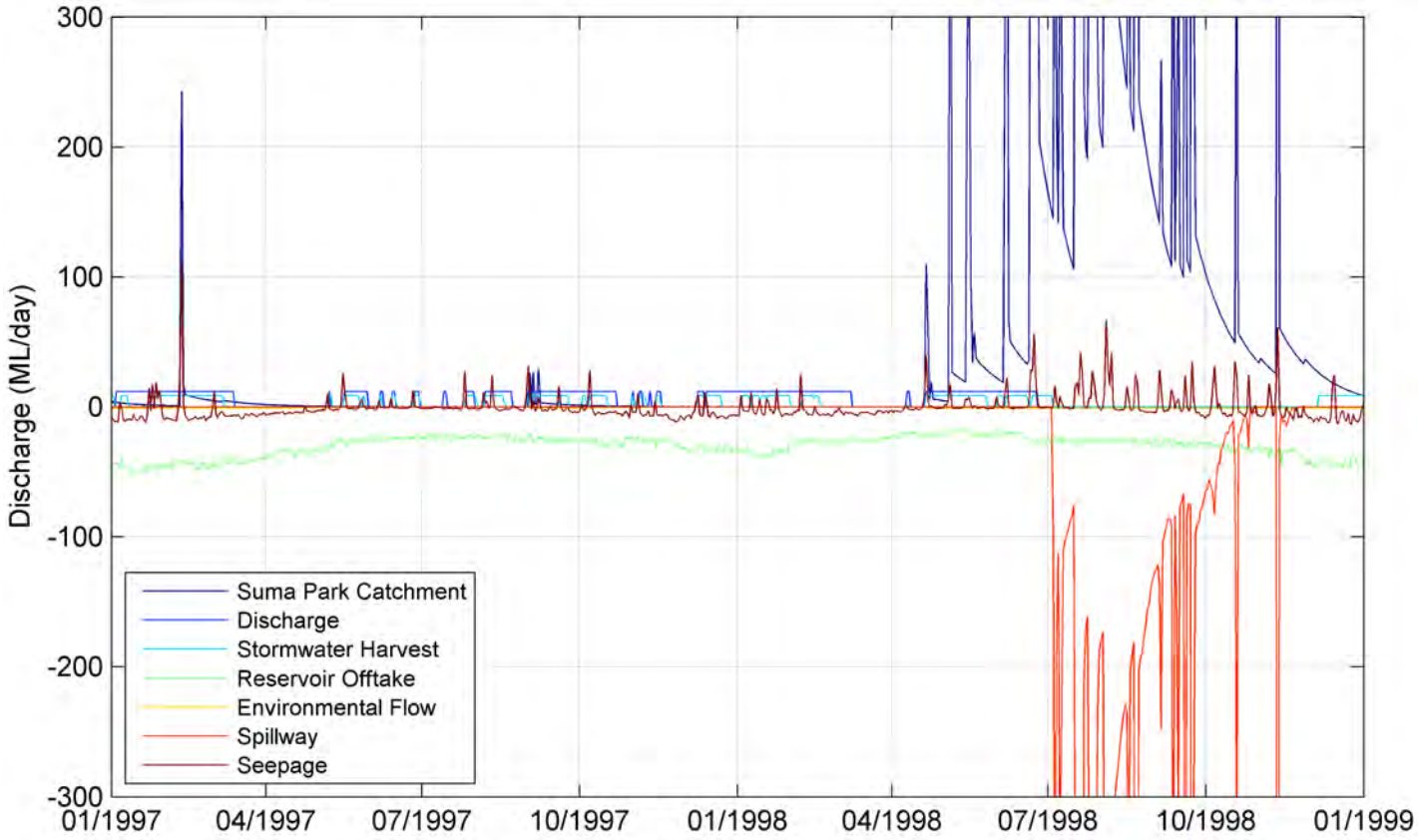
Discharge (ML/day)
300
200
100
0
-100
-200
-300
01/1997
04/1997
07/1997
10/1997
01/1998
04/1998
07/1998
10/1998
01/1999
Suma Park Catchment
Discharge
Stormwater Harvest
Reservoir Offtake
Environmental Flow
Spillway
Seepage

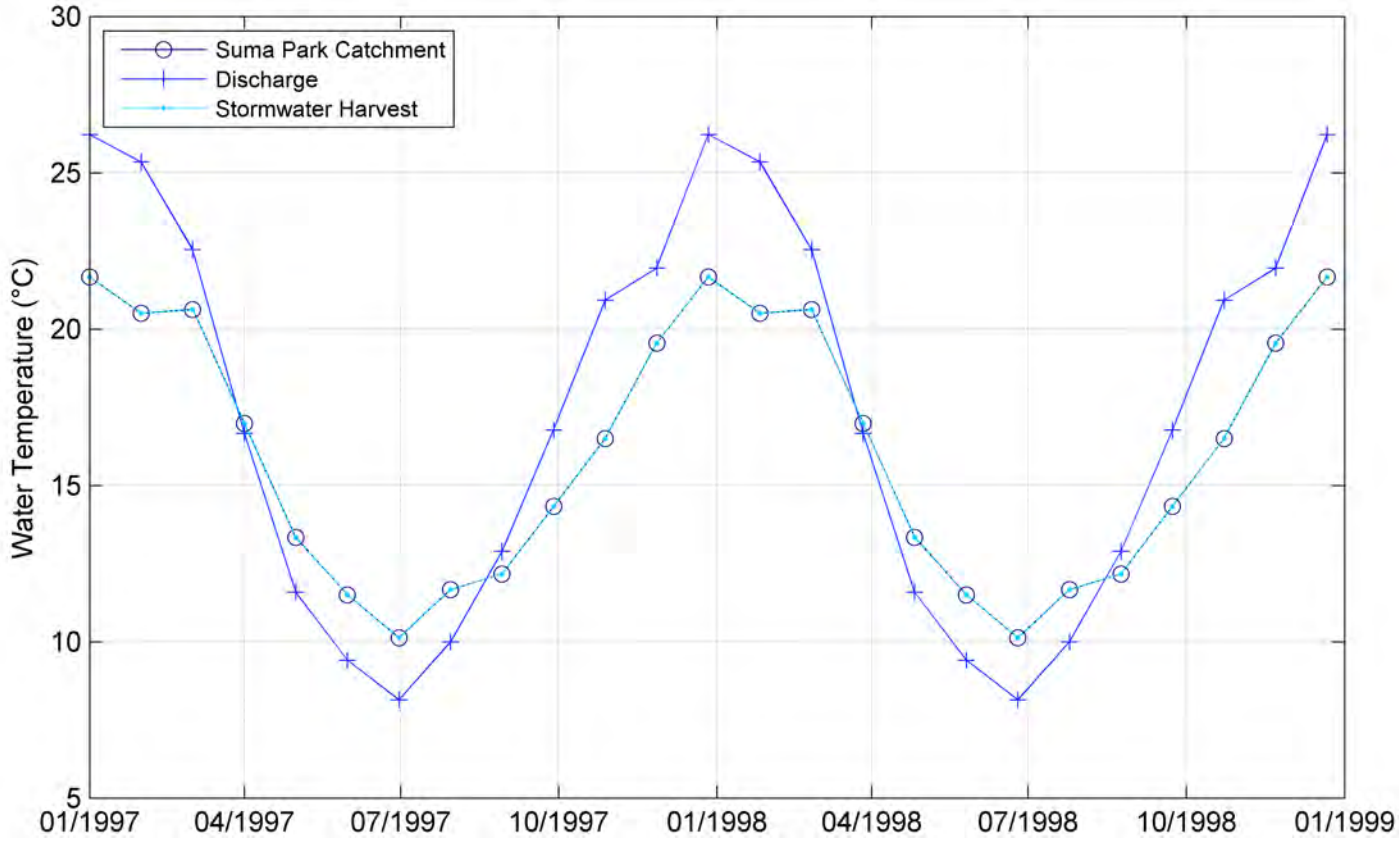
Water Temperature (°C)
30
25
20
15
10
5
01/1997
04/1997
07/1997
10/1997
01/1998
04/1998
07/1998
10/1998
01/1999
Suma Park Catchment
Discharge
Stormwater Harvest

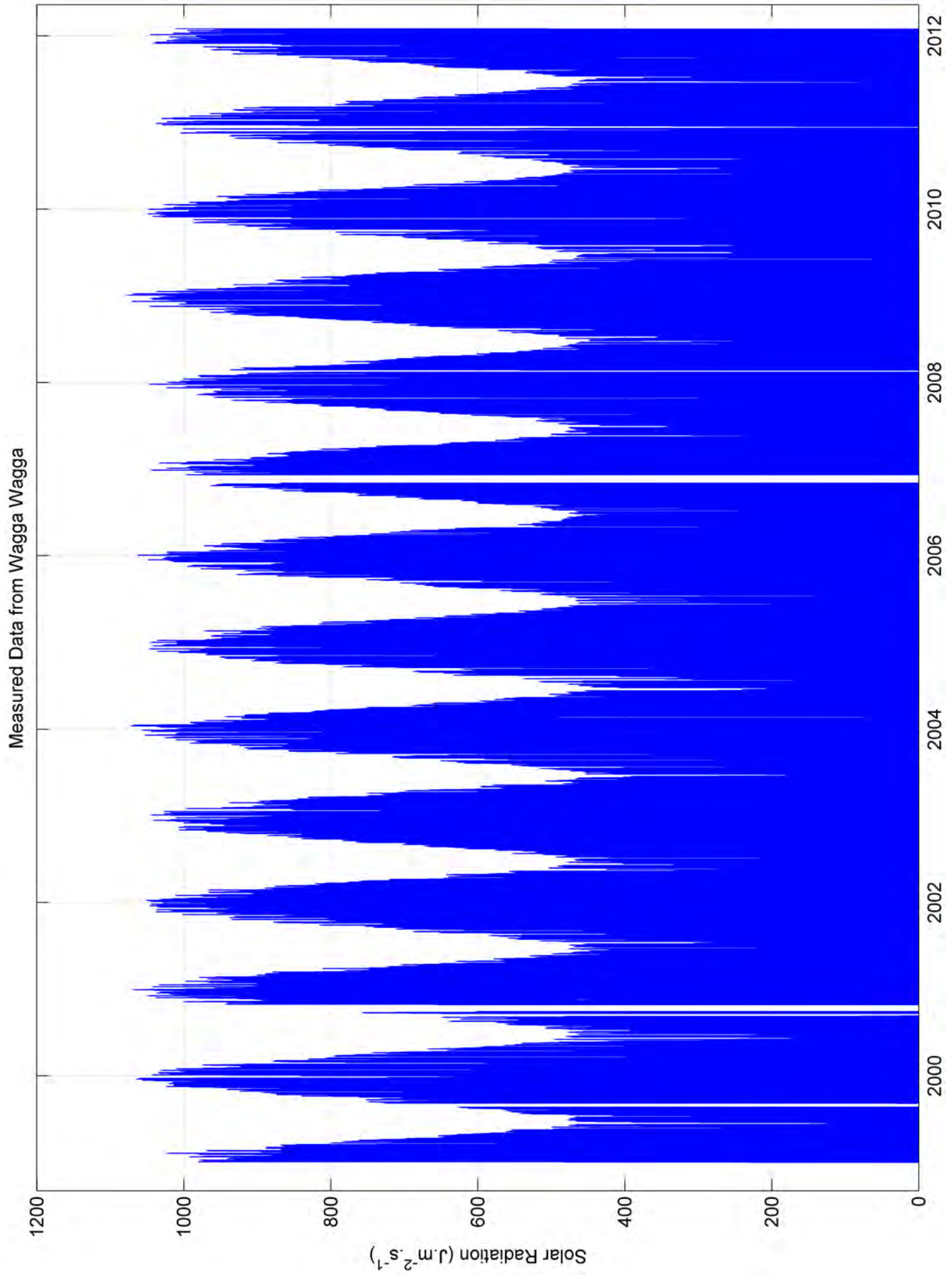

Suma Park Reservoir Numerical Modelling of the Hydro−Thermal Processes and Additional Influx

Cardno

Solar Radiation
Time Series
Figure 3.3a

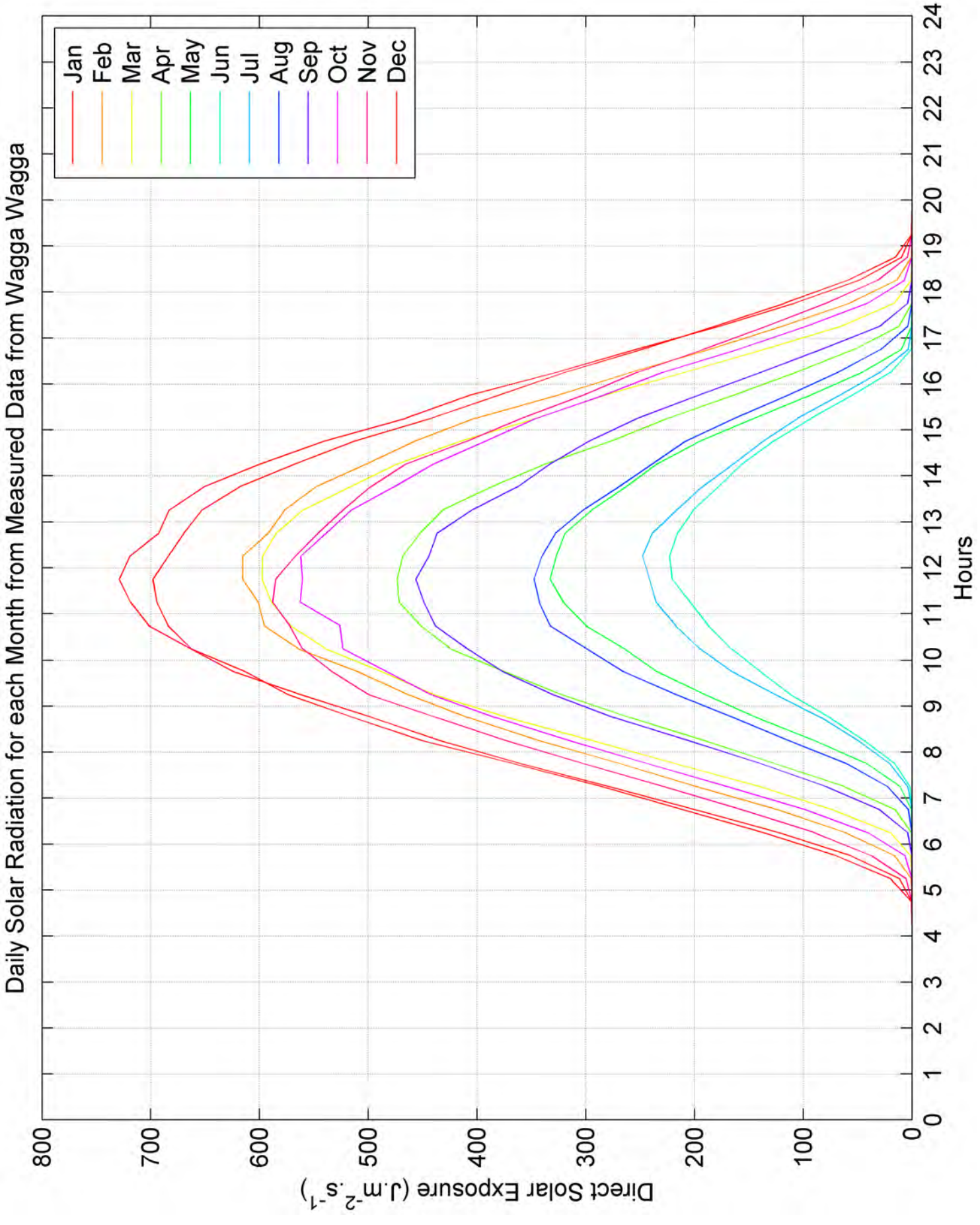
Daily Solar Radiation for each Month from Measured Data from Wagga Wagga
Jan
Feb
Mar
Apr
May
Jun
Jul
Aug
Sep
Oct
Nov
Dec
Direct Solar Exposure (J.m-2.s-1)
800
700
600
500
400
300
200
100
0
Hours
0 1 2 3 4 5 6 7 8 9 10 11 12 13 14 15 16 17 18 19 20 21 22 23 24

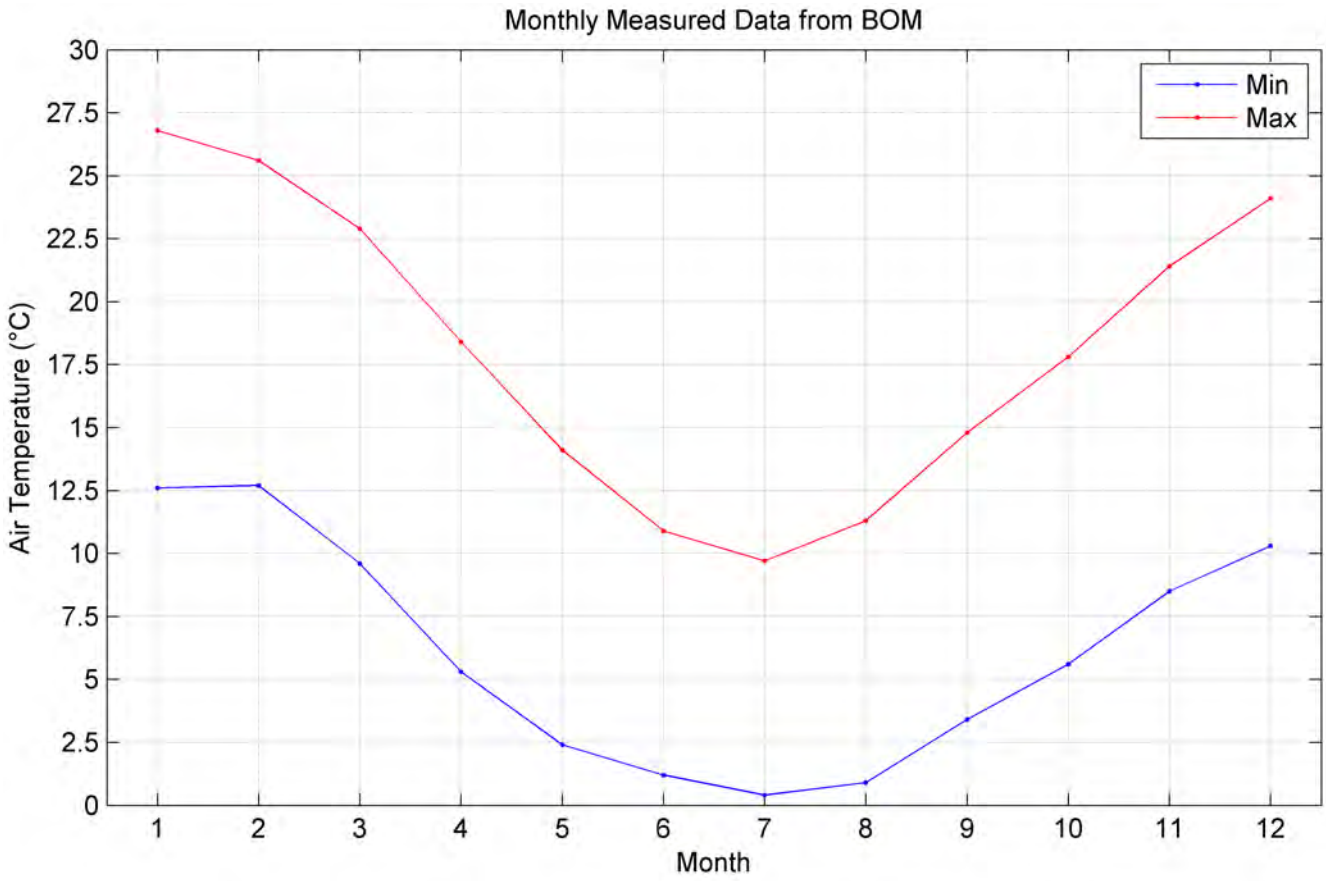
Monthly Measured Data from BOM
Min
Max
Air Temperature (°C)
Month
30
27.5
25
22.5
20
17.5
15
12.5
10
7.5
5
2.5
0
1
2
3
4
5
6
7
8
9
10
11
12

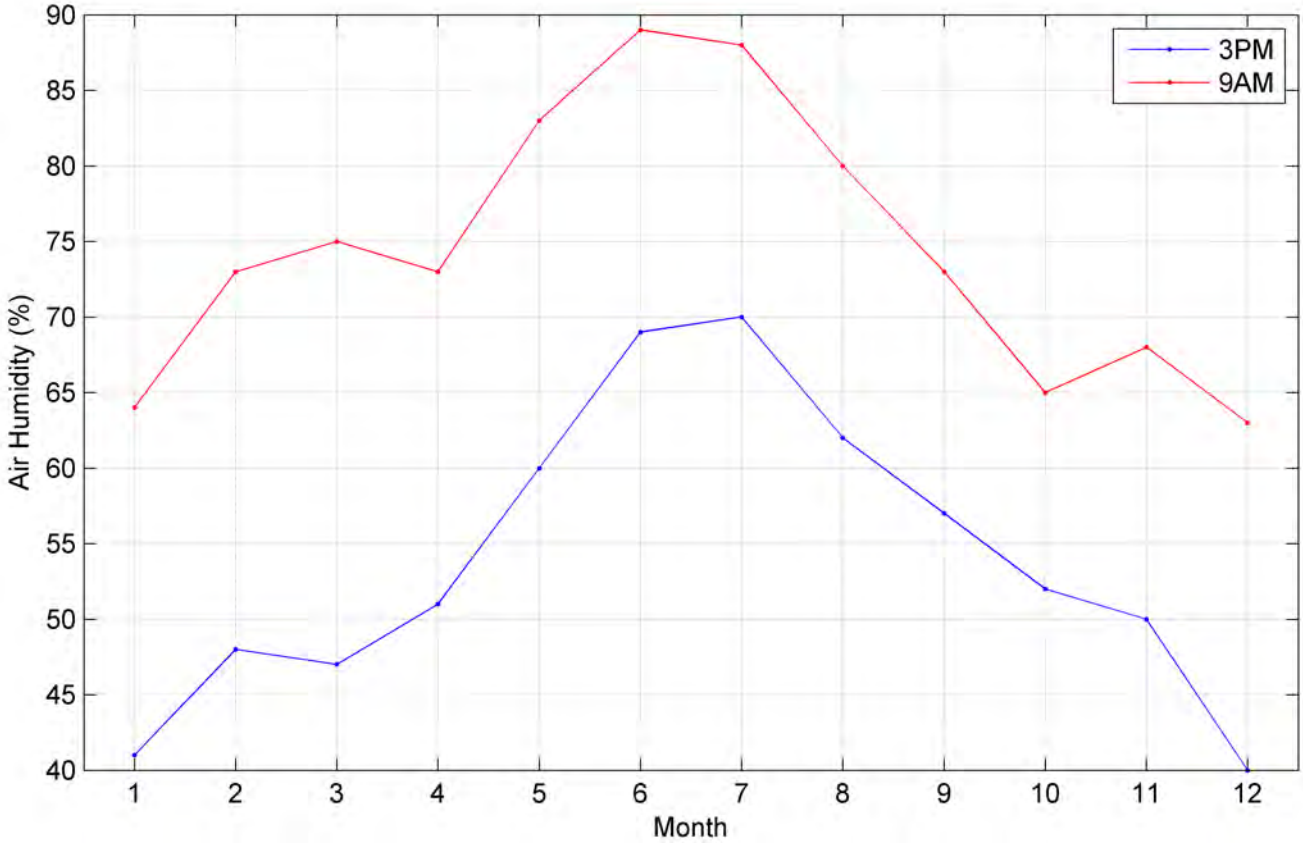
3PM
9AM
Air Humidity (%)
Month
90
85
80
75
70
65
60
55
50
45
40
1
2
3
4
5
6
7
8
9
10
11
12

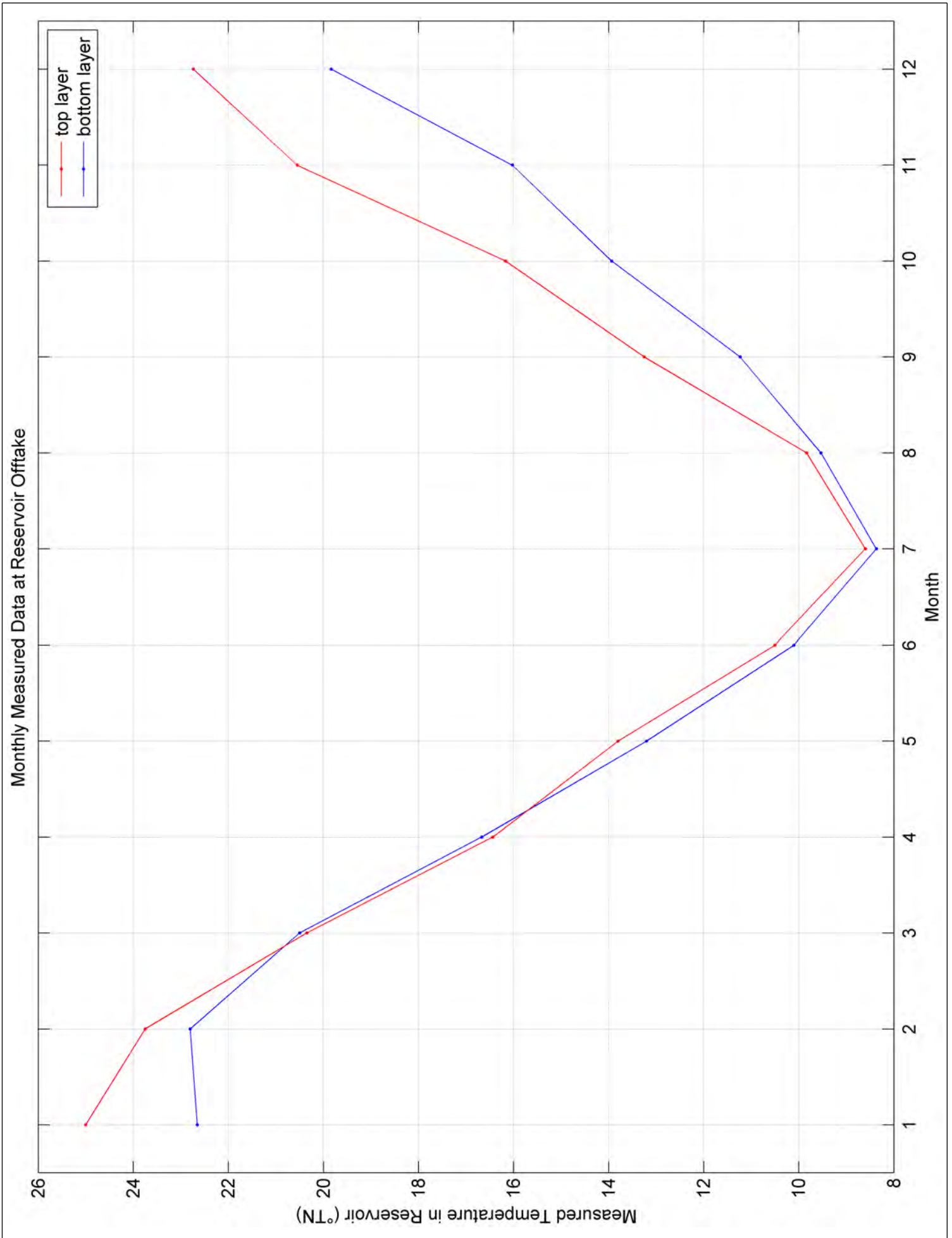

Suma Park Reservoir Numerical Modelling of the Hydro−Thermal Processes and Additional Influx

Water Temperature in Reservoir
Monthly Averages − Surface and Bottom Layers
Figure 3.5

W4916 May 2012
\\Sydcfs01p\Water_Current Projects\4916 Orange Drought Relief Pipeline

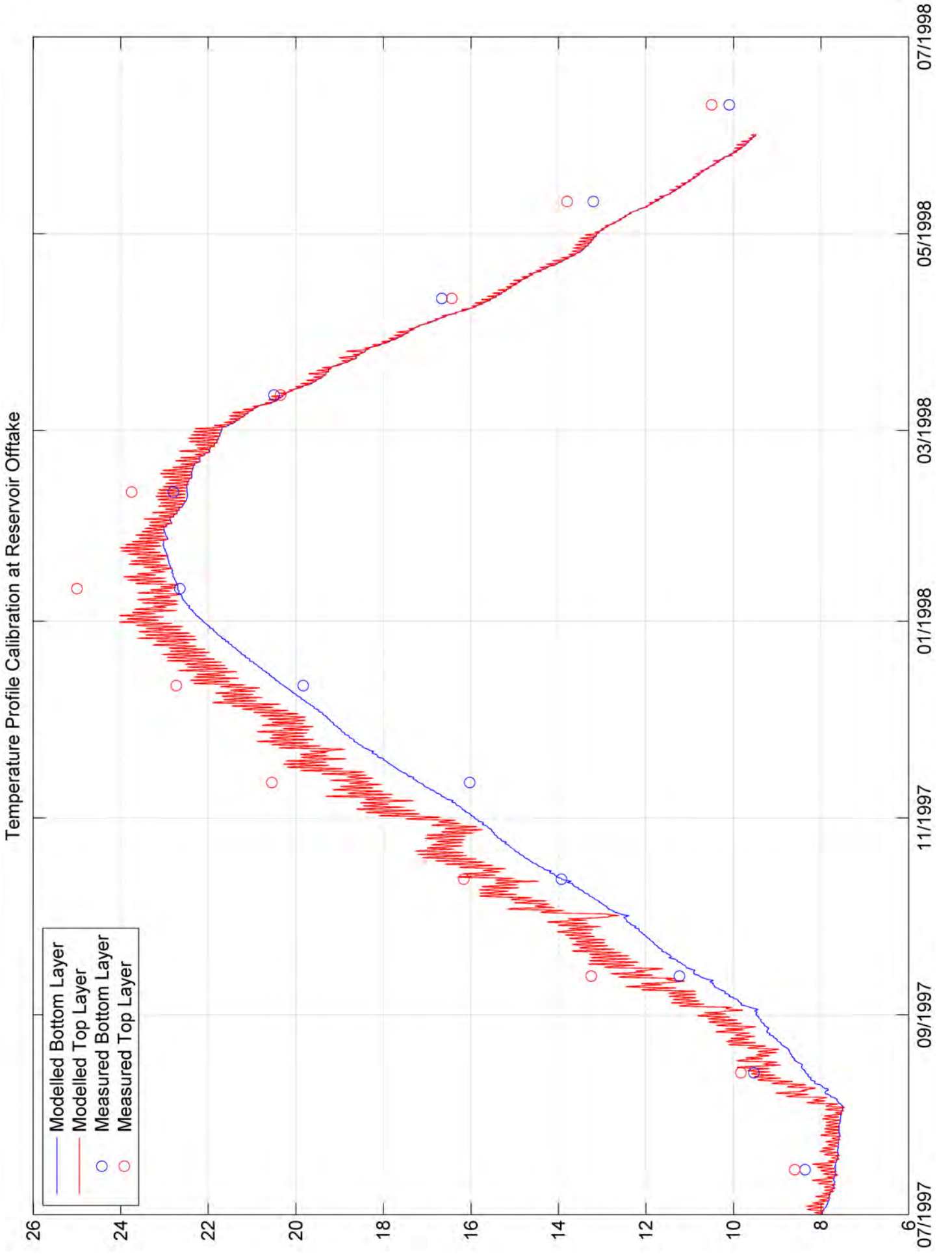

Suma Park Reservoir Numerical Modelling of the Hydro−Thermal Processes and Additional Influx

Cardno

Water Temperature in Reservoir
Model Calibration at Reservoir Offtake
Figure 4.1

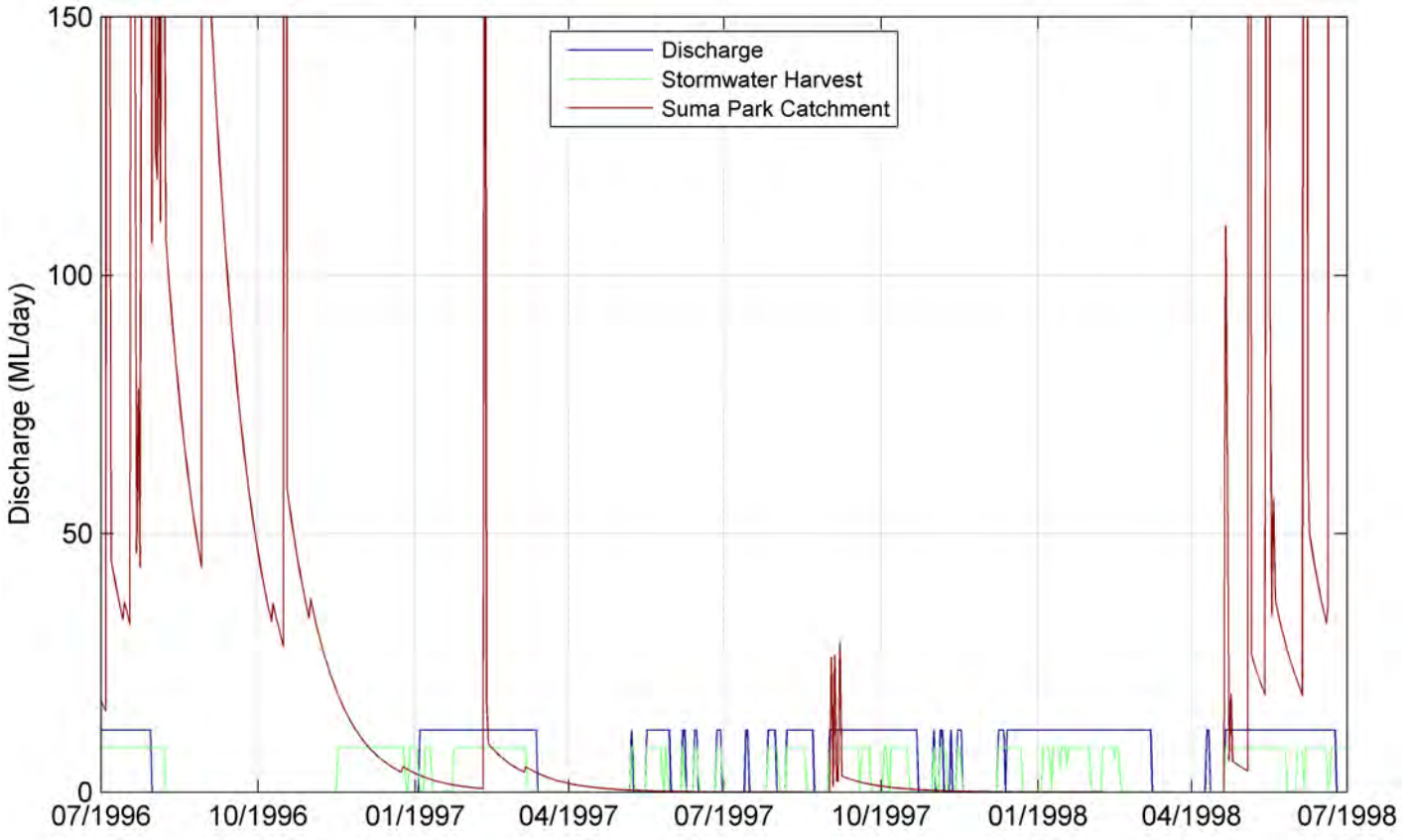

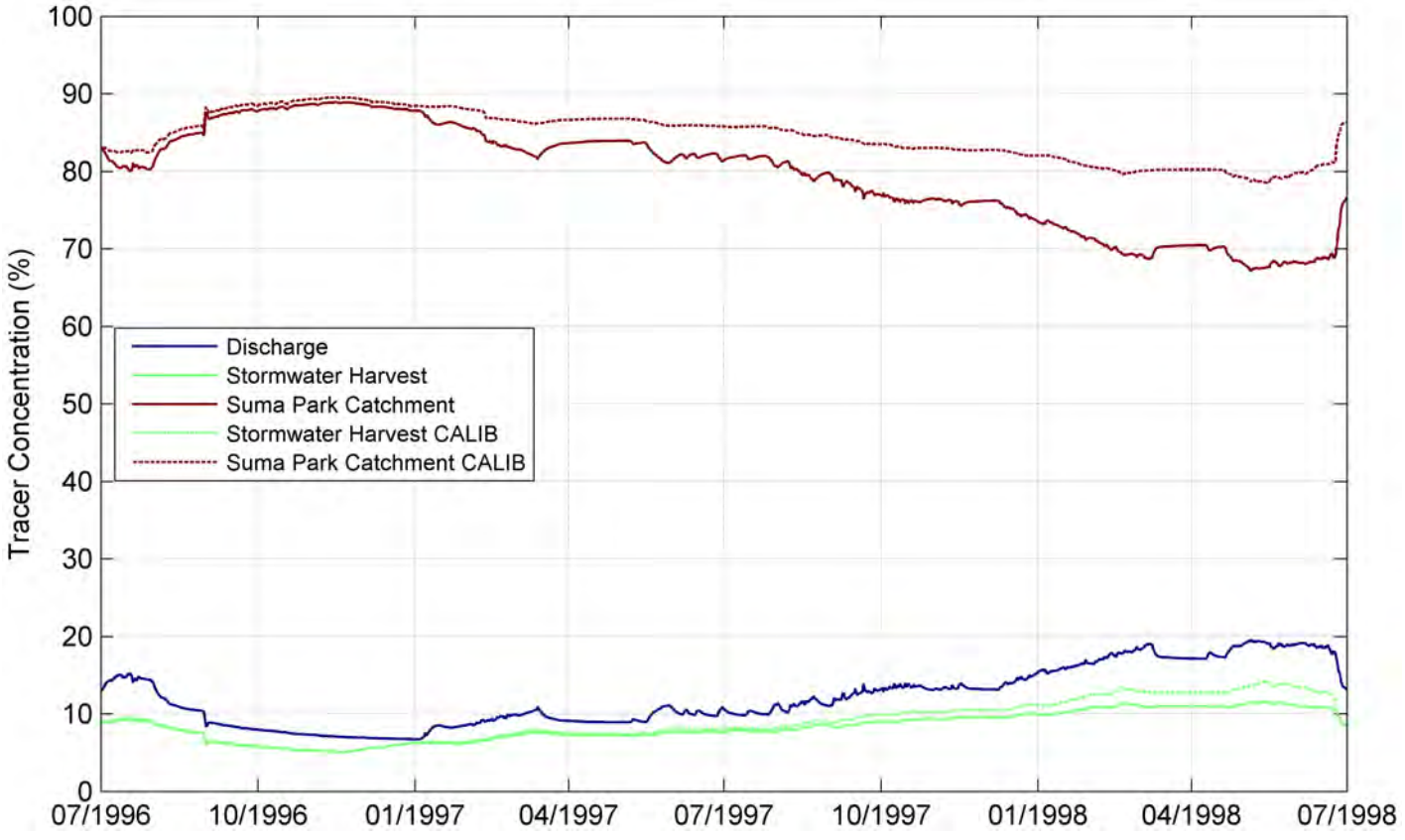

Suma Park Reservoir Numerical Modelling of the Hydro−Thermal Processes and Additional Influx

Cardno

Time Series of Tracer Percentages and Inflow Discharges
07/1996−07/1998
Figure 5.1

W4916 May 2012
\\Sydcfs01p\Water_Current Projects\4916 Orange Drought Relief Pipeline

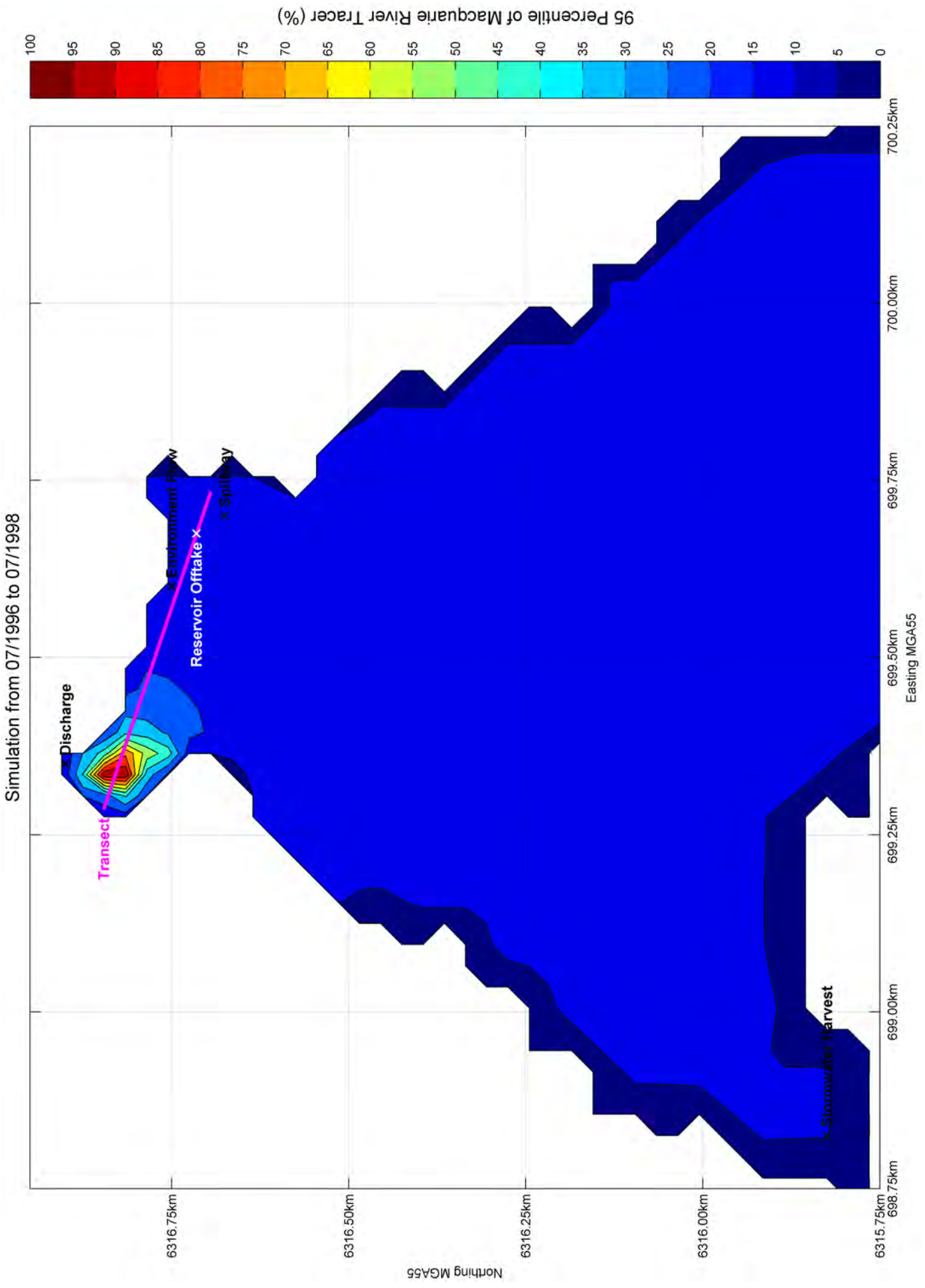

Suma Park Reservoir Numerical Modelling of the Hydro−Thermal Processes and Additional Influx

Spatial Plot of 95 Percentile of Macquarie Tracer Percentage
07/1996−07/1998 − Depth Averaged
Figure 5.2

W4916 May 2012
\\Sydcfs01p\Water_Current Projects\4916 Orange Drought Relief Pipeline

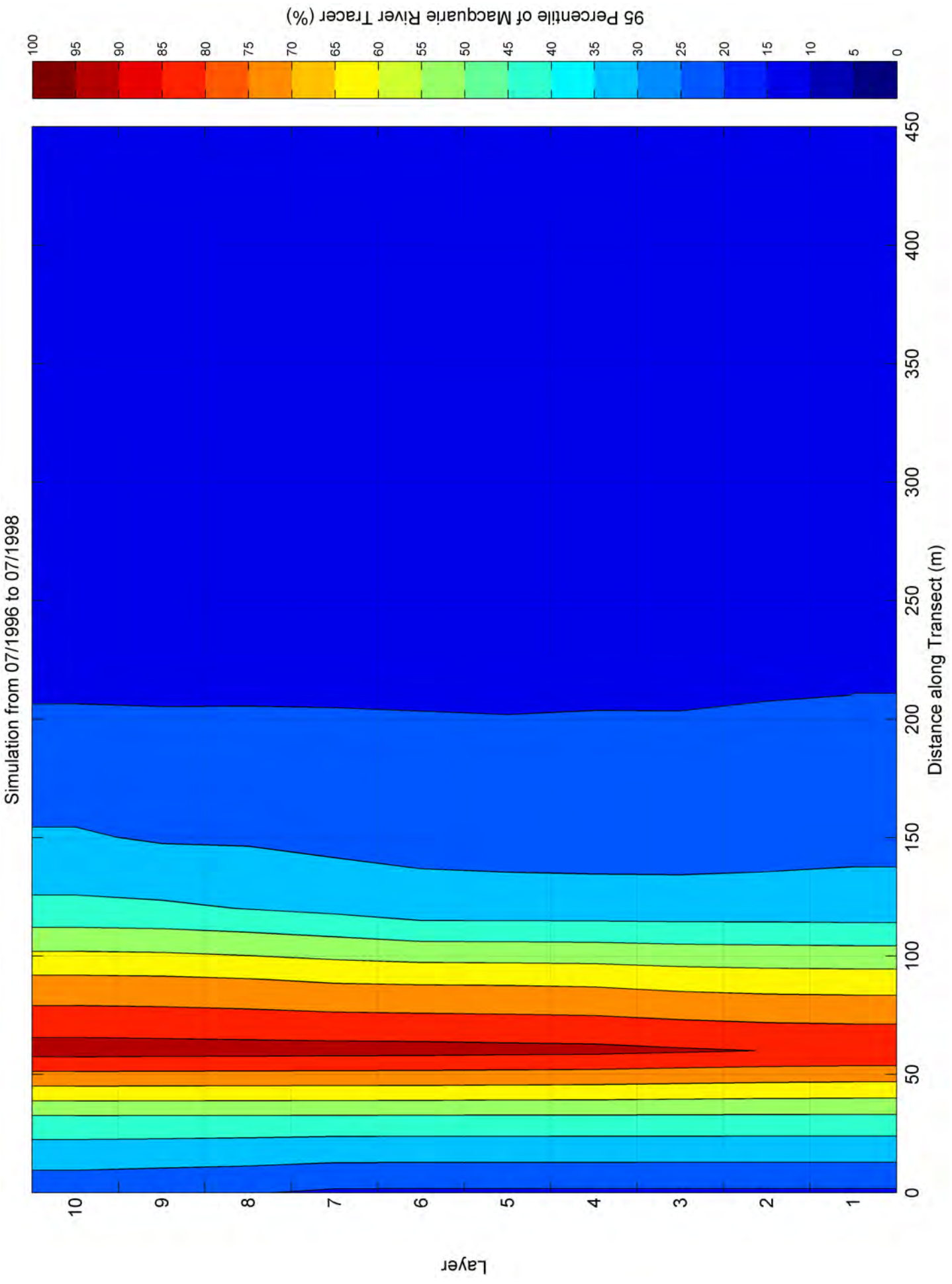

Suma Park Reservoir Numerical Modelling of the Hydro−Thermal Processes and Additional Influx

Cardno

Transect of 95 Percentile of Macquarie River Tracer Percentage
07/1996−07/1998 − 10 Depth Layers
Figure 5.3

W4916 May 2012
\\Sydcfs01p\Water_Current Projects\4916 Orange Drought Relief Pipeline

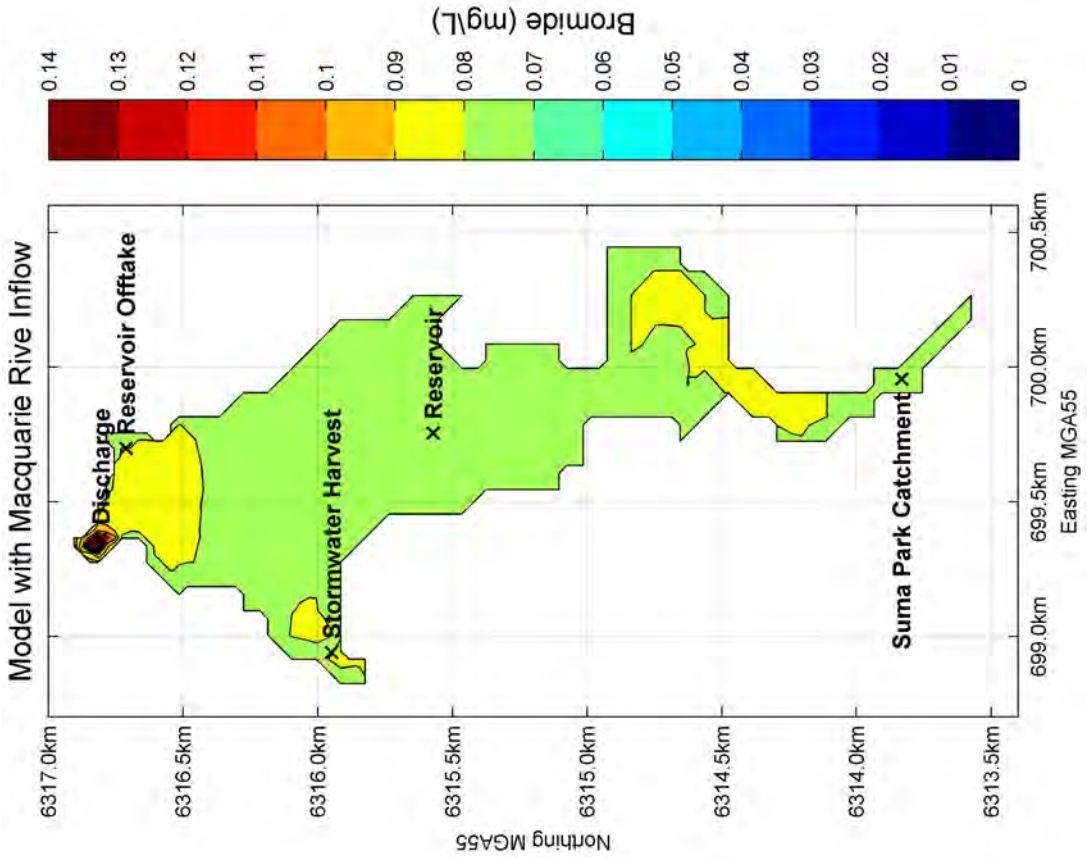
Model with Macquarie Rive Inflow
Bromide (mg\L)
0.14
0.13
0.12
0.11
0.1
0.09
0.08
0.07
0.06
0.05
0.04
0.03
0.02
0.01
0
Discharge
Reservoir Offtake
Reservoir
Stormwater Harvest
Suma Park Catchment
6317.0km
6316.5km
6316.0km
6315.5km
6315.0km
6314.5km
6314.0km
6313.5km
Northing MGA55
699.0km
699.5km
700.0km
700.5km
Easting MGA55

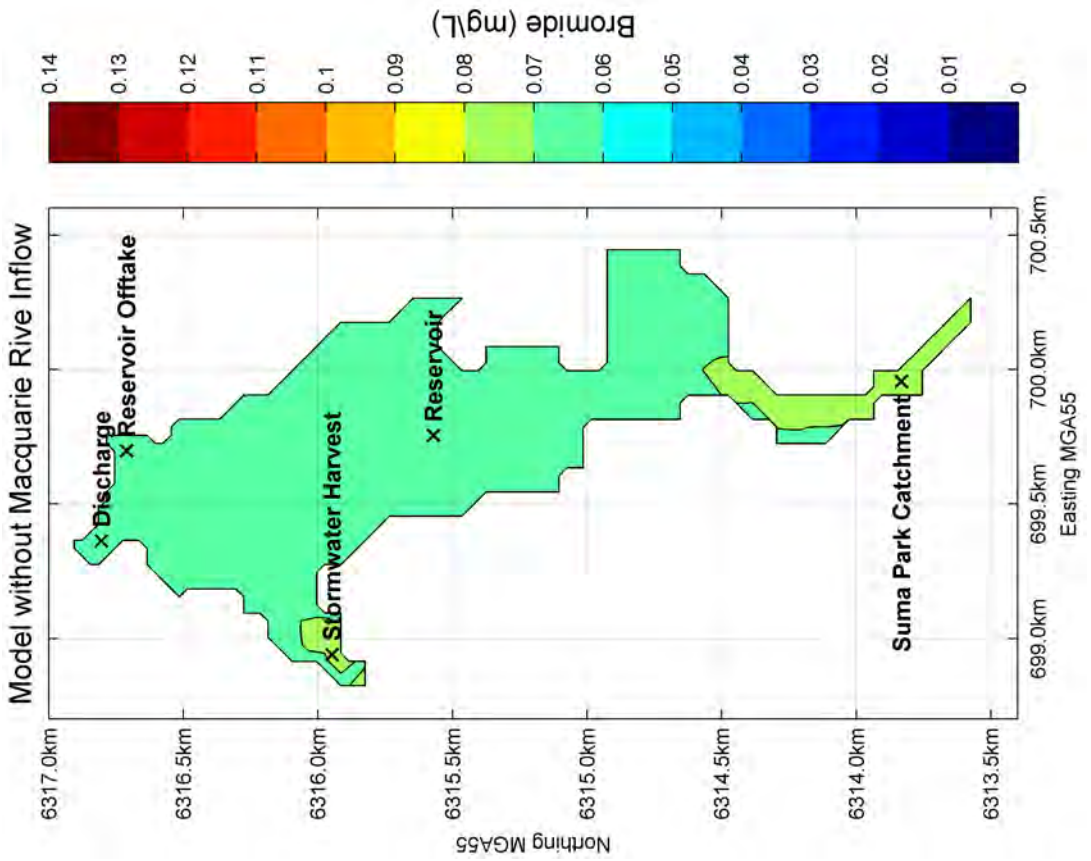
Model without Macquarie Rive Inflow
Bromide (mg\L)
0.14
0.13
0.12
0.11
0.1
0.09
0.08
0.07
0.06
0.05
0.04
0.03
0.02
0.01
0
Discharge
Reservoir Offtake
Reservoir
Stormwater Harvest
Suma Park Catchment
6317.0km
6316.5km
6316.0km
6315.5km
6315.0km
6314.5km
6314.0km
6313.5km
Northing MGA55
699.0km
699.5km
700.0km
700.5km
Easting MGA55

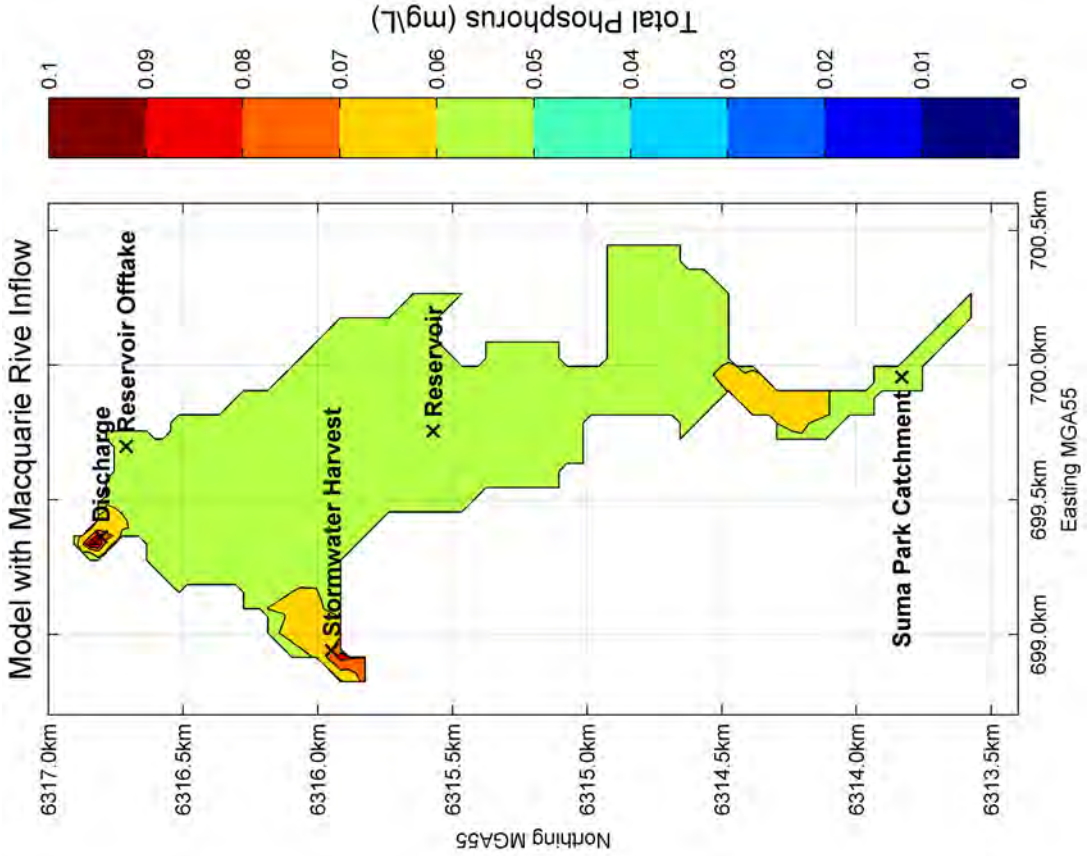

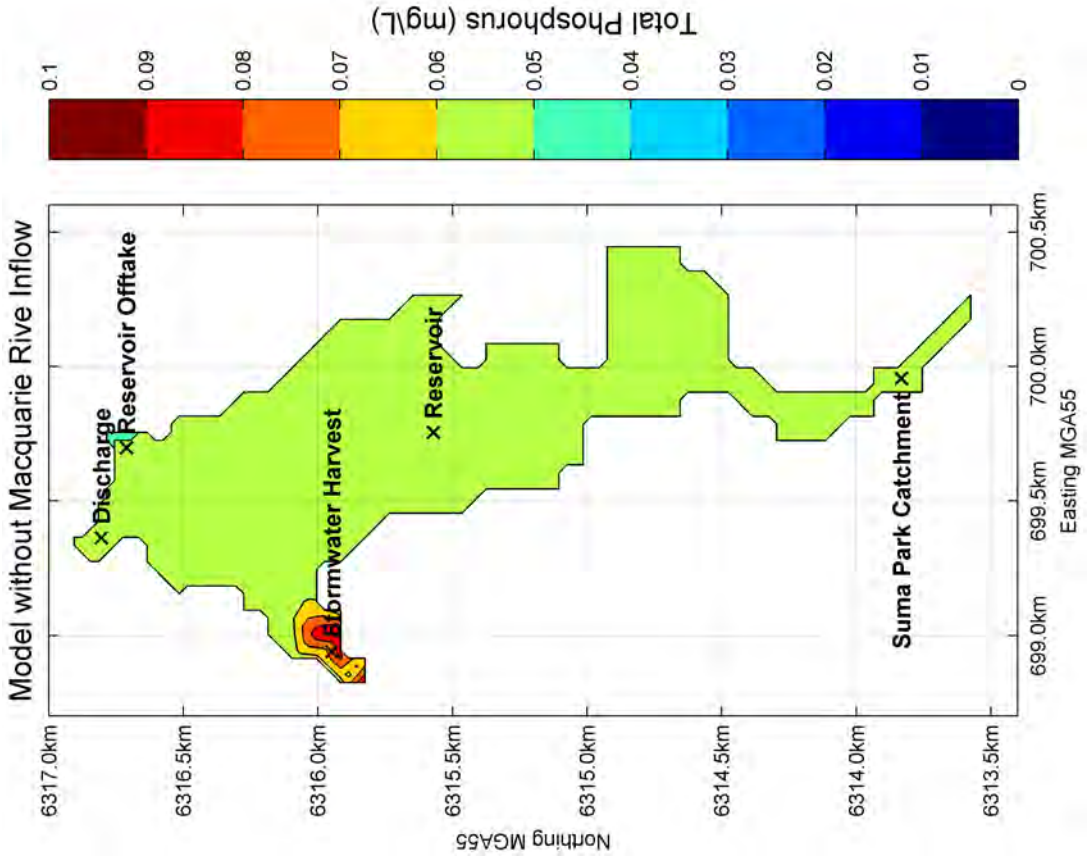

Suma Park Reservoir Numerical Modelling of the Hydro−Thermal Processes and Additional Influx

Cardno

95 Percentile Concentration Plot
Total Nitrogen − 07/1996−07/1998
Figure 5.4b

W4916 May 2012
\\Sydcfs01p\Water_Current Projects\4916 Orange Drought Relief Pipeline

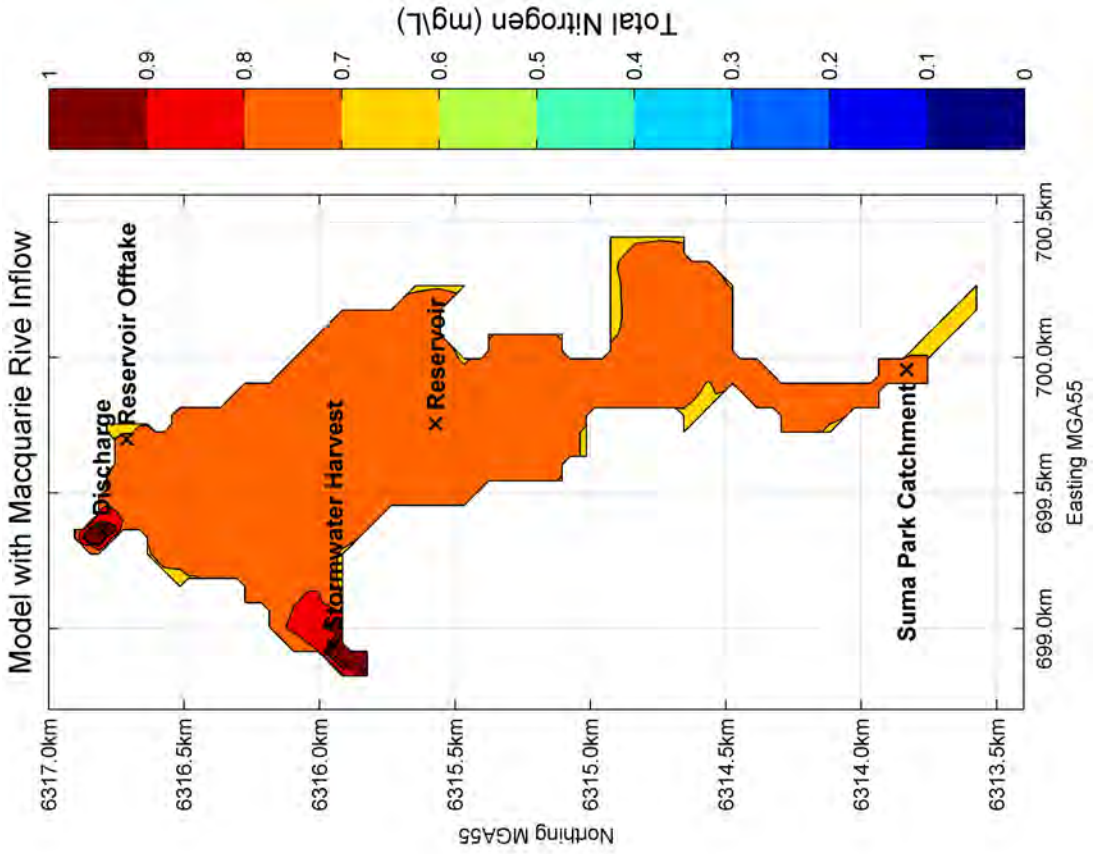

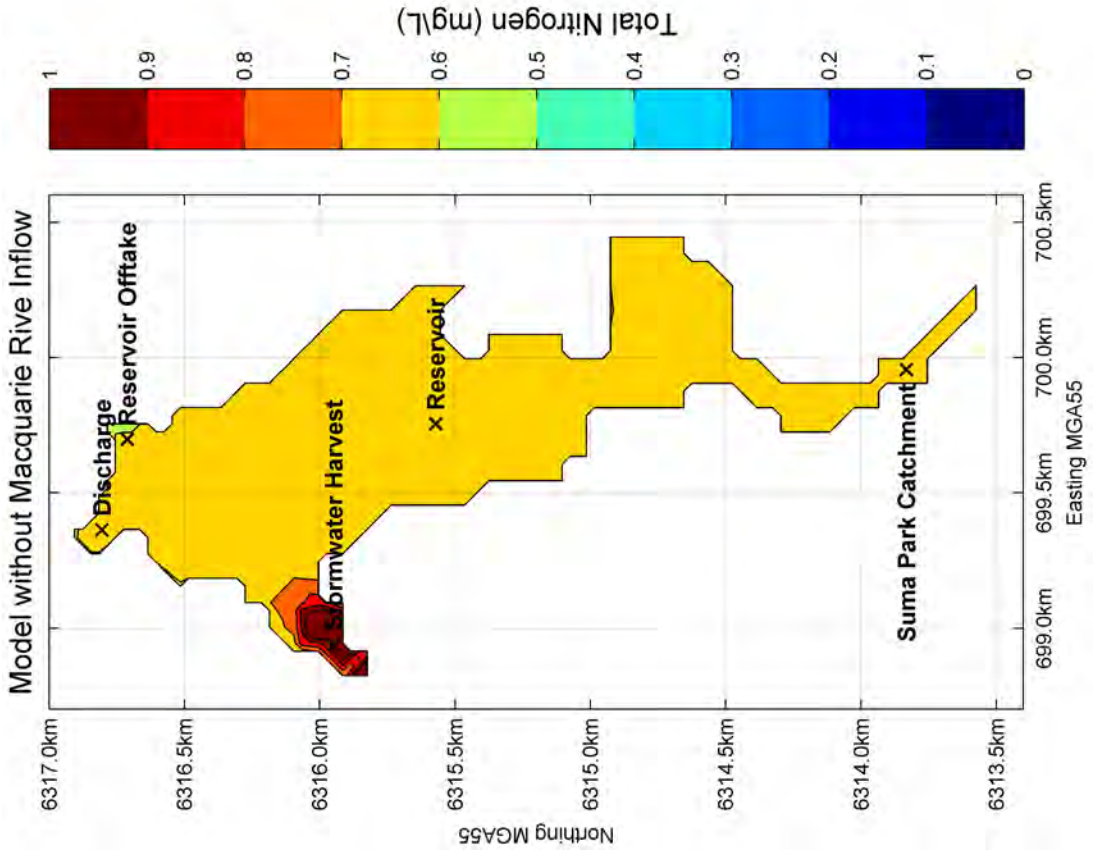

Suma Park Reservoir Numerical Modelling of the Hydro−Thermal Processes and Additional Influx

Cardno

95 Percentile Concentration Plot
Total Phosphorus − 07/1996−07/1998
Figure 5.4c

W4916 May 2012
\\Sydcfs01p\Water_Current Projects\4916 Orange Drought Relief Pipeline

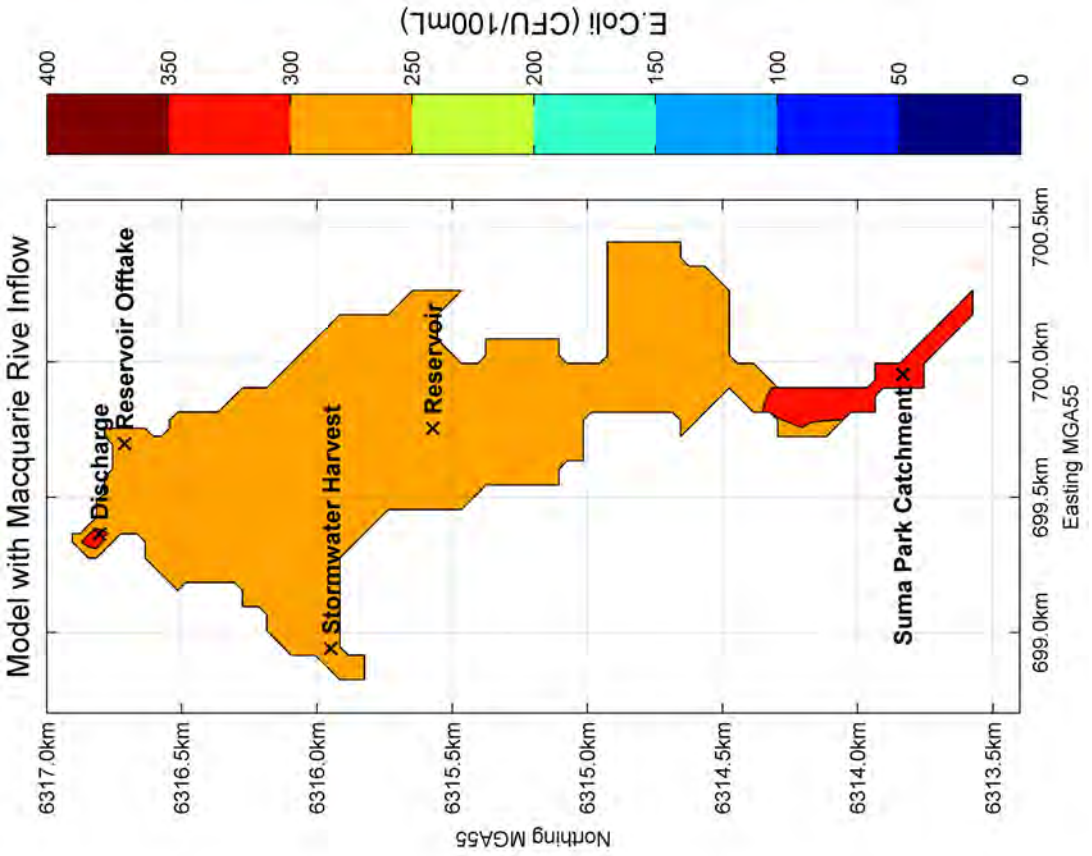
Model with Macquarie Rive Inflow
E.Coli (CFU/100mL)
400
350
300
250
200
150
100
50
0
Discharge
Reservoir Offtake
Stormwater Harvest
Reservoir
Suma Park Catchment
6317.0km
6316.5km
6316.0km
6315.5km
6315.0km
6314.5km
6314.0km
6313.5km
Northing MGA55
699.0km
699.5km
700.0km
700.5km
Easting MGA55

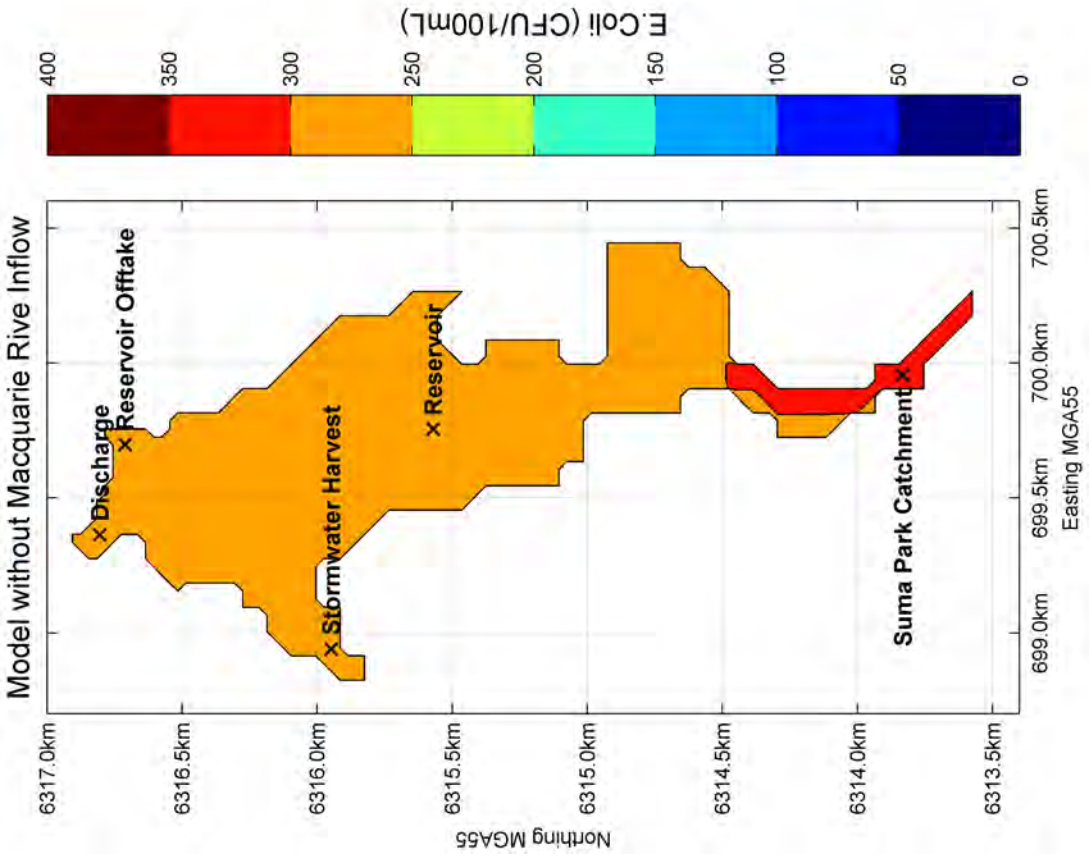
Model without Macquarie Rive Inflow
E.Coli (CFU/100mL)
400
350
300
250
200
150
100
50
0
Discharge
Reservoir Offtake
Stormwater Harvest
Reservoir
Suma Park Catchment
6317.0km
6316.5km
6316.0km
6315.5km
6315.0km
6314.5km
6314.0km
6313.5km
Northing MGA55
699.0km
699.5km
700.0km
700.5km
Easting MGA55